HTR10-GCR-RESR-001
CRIT

EVALUATION OF THE INITIAL CRITICAL CONFIGURATION OF THE HTR-10 PEBBLE-BED REACTOR

Evaluator

William K. Terry
Idaho National Laboratory

Internal Reviewers

Soon-Sam Kim
J. Blair Briggs

Independent Reviewers

Yuliang Sun
Institute of Nuclear Energy Technology
Tsinghua University

Temitope Tiawo
Argonne Laboratory

Status of Compilation / Evaluation / Peer Review

Chapter	Page	Compiled	Independent Review	Working Group Review	Approved
1.0 DETAILED DESCRIPTION	4				
1.1 Description of the Critical and / or Subcritical Configuration	6				
1.2 Description of Buckling and Extrapolation Length Measurements	16				
1.3 Description of Spectral Characteristics Measurements	16				
1.4 Description of Reactivity Effects Measurements	16				
1.5 Description of Reactivity Coefficient Measurements	16				
1.6 Description of Kinetics Measurements	16				
1.7 Description of Reaction-Rate Distribution Measurements	16				
1.8 Description of Power Distribution Measurements	16				
1.9 Description of Isotopic Measurements	16				
1.10 Description of Other Miscellaneous Types of Measurements	16				
Chapter	**Page**	**Evaluated**	**Independent Review**	**Working Group Review**	**Approved**
2.0 EVALUATION OF EXPERIMENTAL DATA	17				
2.1 Evaluation of Critical and / or Subcritical Configuration Data	19				
2.2 Evaluation of Buckling and Extrapolation Length Data	38				
2.3 Evaluation of Spectral Characteristics Data	38				
2.4 Evaluation of Reactivity Effects Data	38				
2.5 Evaluation of Reactivity Coefficient Data	38				
2.6 Evaluation of Kinetics Measurements Data	38				
2.7 Evaluation of Reaction Rate Distributions	38				
2.8 Evaluation of Power Distribution Data	38				
2.9 Evaluation of Isotopic Measurements	38				
2.10 Evaluation of Other Miscellaneous Types of Measurements	38				

Chapter	Page	Compiled	Independent Review	Working Group Review	Approved
3.0 BENCHMARK SPECIFICATIONS	39				
3.1 Benchmark-Model Specifications for Critical and / or Subcritical Measurements	39				

EVALUATION OF THE INITIAL CRITICAL CONFIGURATION OF THE HTR-10 PEBBLE-BED REACTOR

IDENTIFICATION NUMBER: HTR10-GCR-RESR-001
CRIT

KEY WORDS: Pebble-bed reactor, criticality, research reactor, benchmark evaluation, Chinese Reactors, HTR-10, graphite-moderated reactors, HTGRs

1.0 DETAILED DESCRIPTION

The HTR-10 is a small (10 MWt) pebble-bed research reactor intended to develop pebble-bed reactor (PBR) technology in China. It will be used to test and develop fuel, verify PBR safety features, demonstrate combined electricity production and co-generation of heat, and provide experience in PBR design, operation, and construction.

Table 1 gives major design features of the reactor, and Figure 1 illustrates the reactor layout. The reactor was not at power during the subject experiment, and some key features, such as the composition of the gas in the void spaces, were different from the specifications in Table 1, as explained in detail below. However, the data in Table 1 serve to characterize the reactor, and they are therefore included here.

Table 1. Reactor design features (from Reference 1)

Reactor thermal power	MW	10
Primary helium pressure	MPa	3.0
Reactor core diameter	cm.	180
Average core height	cm.	197
Average helium temperature at reactor outlet	°C	700
Average helium temperature at reactor inlet	°C	250
Helium mass flow rate at full power	kg/s	4.3
Main steam pressure at steam generator outlet	MPa	4.0
Main steam temperature at steam generator outlet	°C	440
Feed water temperature	°C	104
Main steam flow rate	t/hr	12.5
Number of control rods in side reflector		10
Number of absorber ball units in side reflector		7
Nuclear fuel		UO_2
Heavy metal loading per fuel element	g	5
Enrichment of fresh fuel element	%	17
Number of fuel elements in equilibrium core		27,000
Fuel loading mode		multi-pass

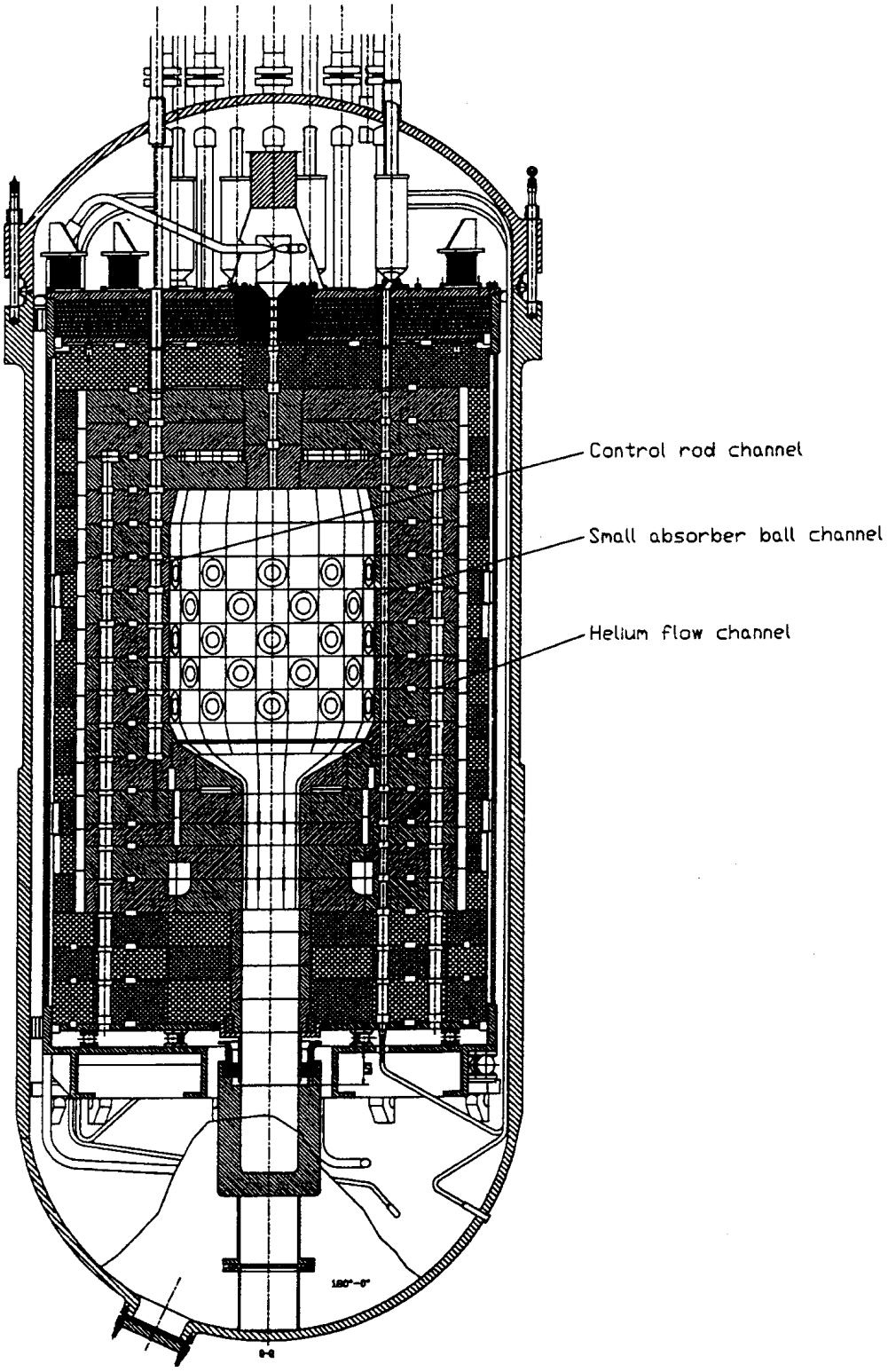

Figure 1. Layout of HTR-10 (from Reference 1)

As a test reactor intended to demonstrate all the technologies associated with PBRs, the HTR-10 contains a complete cooling system that supplies hot helium to a steam generator for generation of electricity and supply of district heating. In a later experimental phase, the HTR-10 will supply heat to both a steam cycle and a gas-turbine cycle. The primary coolant loop contains three pressure vessels: the reactor vessel, the steam generator vessel, and the hot gas duct. In the initial criticality experiment, only the core and the reflector are modeled.

The HTR-10 first became critical on 1 December 2000. This evaluation assesses the usefulness of the data obtained in the initial criticality experiment as a benchmark for reactor physics codes. It is concluded that the experiment is an acceptable benchmark.

In the initial critical condition, all control rods were withdrawn. Measurements of control rod worth were also made on the cold clean core. The control rod worth experiments have not yet been evaluated.

1.1 Description of the Critical Configuration

Like any PBR, the HTR-10 is fueled by billiard-ball-size spheres containing fuel particles embedded in a matrix. During reactor operation, the fuel spheres are introduced at the top and slowly flow downwards through the core region. As shown in Figure 1, the HTR-10 core is a cylindrical cavity above a conical zone (the "conus") that funnels pebbles into a discharge tube. The core, conus, and discharge tube are surrounded by graphite blocks (the reflector), most of which contain boron and some of which are penetrated by various borings for coolant flow, control rods, emergency shutdown absorber balls, and other purposes. In the initial critical experiment, the voids in the core and reflector were filled by moist air rather than the helium with which the reactor is cooled while in operation, and the conus was filled with "dummy" balls – spheres the same size as fuel spheres but made only of graphite. In the cylindrical core, a mixture of fuel balls and dummy balls in the ratio of 57:43 was added until the core became critical. During this initial fuel loading, pebbles were not removed at the bottom, so the pebbles remained stationary after they settled into position in the core. A small Am-Be source (4.4×10^7 neutrons/s) was provided to assist startup, and the neutron flux was tracked by neutron counters. Criticality was achieved when 16,890 balls (fuel and dummy) had been loaded. This is equivalent to a level core height of 123.06 cm.

1.1.1 Overview of Experiment

The HTR-10 is located at the Institute of Nuclear Energy Technology (INET), a unit of Tsinghua University, near Beijing. The HTR-10 project was approved by the Chinese State Council in March 1992, ground was broken in 1994, and construction was

completed in 2000. Initial criticality was achieved on 1 December 2000. The experiment was performed by the INET, led by Professor Yuliang Sun.

In advance of the actual experiment, data were distributed worldwide for interested groups to use in benchmarking calculations with various computer codes. The benchmark problem specifications differed in several respects from the experiment as it was run. Some compositions provided in the benchmark specifications were different from the as-built compositions, the benchmark and as-run temperatures were different, and the void spaces in the actual experiment were filled with air instead of helium. The results of the benchmark efforts are reported in Reference 1.

The initial criticality experiment has a total uncertainty in k_{eff} of slightly more than 0.005. It is judged acceptable as a benchmark.

1.1.2 Description of Experimental Configuration

Dimensions and material data describing the initial critical experiment were provided by the HTR-10 research group in Reference 1. Dimensional data are presented in this subsection, and material data are provided in the next one. Figure 2 shows the construction of the fuel pebble and the TRISO fuel particles embedded in the fuel zone matrix of the fuel pebble. Table 2 shows the dimensions of the various components of the fuel pebble and fuel particle illustrated in Figure 2. Table 3 shows the nominal dimensions of all components in the core and reflector, together with tolerance limits, observed ranges, and standard deviations where they are known. The nominal compositions are taken from Reference 1, and the uncertainties are taken from Reference 2. Reference 2 presents data obtained by 1997, so it might not reflect tolerances or observations in the year of the experiment, but it contains the only information found on the tolerance specifications for the HTR-10.

Table 2. Dimensions of Pebbles and Fuel Particles

Diameter of ball	6.0 cm
Diameter of fuel zone	5.0 cm
Volumetric filling fraction of balls in the core	0.61
Radius of the kernel(mm)	0.25
Coating layer materials (starting from kernel)	Buffer/PyC/SiC/PyC
Coating layer thickness(mm)	0.09/0.04/0.035/0.04
Diameter of dummy (no fuel) elements	6.0 cm

As noted above, the reflector region comprises numerous graphite blocks of different compositions. The variations in the volume-averaged compositions of the blocks arise both from different boron concentrations and from different sizes and placements of borings. Reference 1 contains a mapping of the various blocks into model regions, with

average material densities provided. This mapping, with dimensions shown, is presented in Figure 3; this figure differs slightly from the analogous figure in Reference 1, as explained in Section 3.

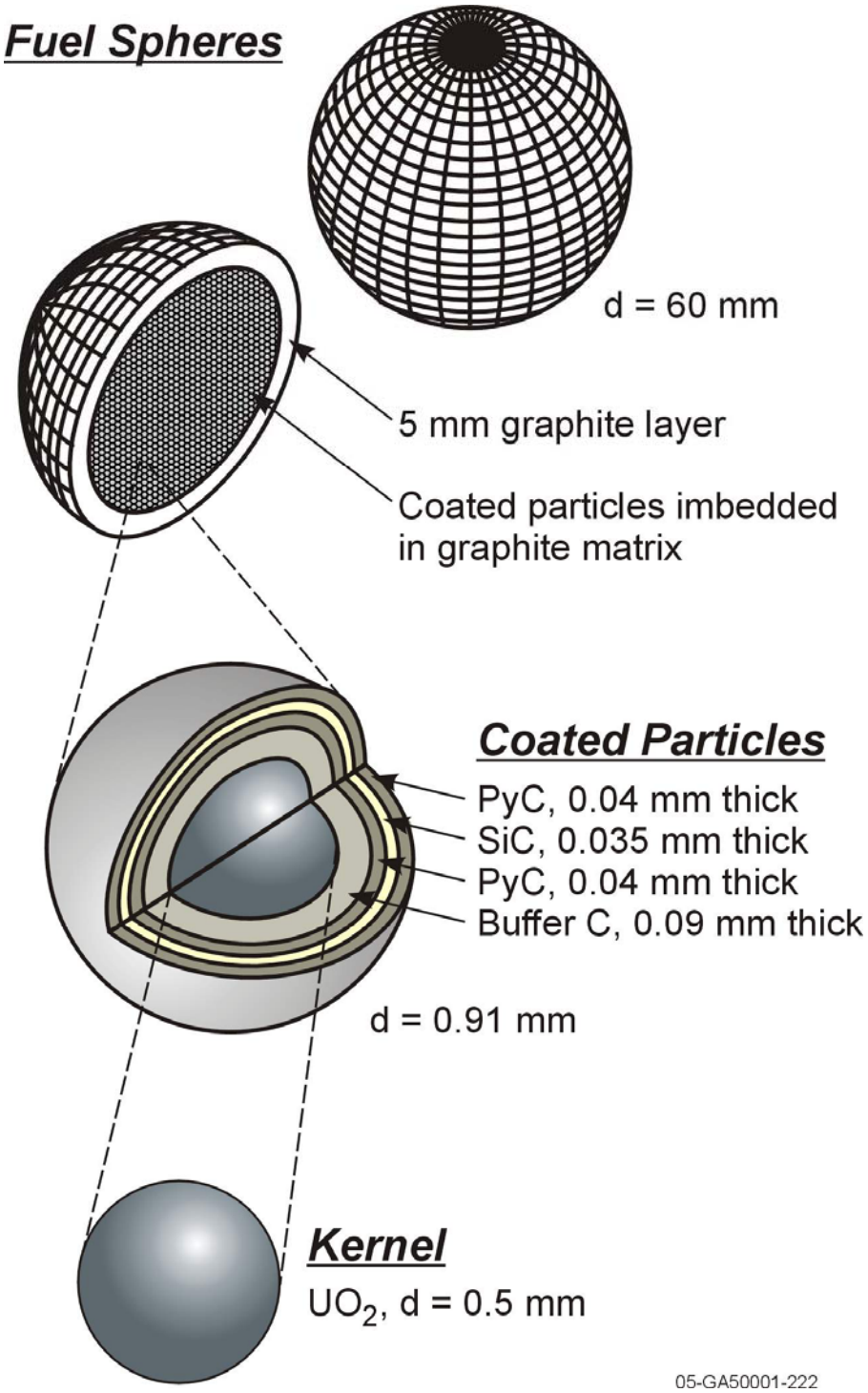

Figure 2. Illustration of Fuel Spheres and TRISO Coated Particles

Table 3. Nominal values and variations in dimensions

Item	Nominal Value	Design Tolerances	Observed Range	Standard Deviation
Core height	123 cm	n/a	n/a	n/a
Diameter of core cavity	180 cm	n/a	n/a	n/a
Height of core cavity	221.818 cm	n/a	n/a	n/a
Height of conus	36.946 cm	n/a	n/a	n/a
Dimensions of graphite blocks	Various	n/a	n/a	n/a
Outer diameter of graphite reflector	380.0 cm	n/a	n/a	n/a
Overall height of graphite reflector	610.0 cm	n/a	n/a	n/a
Diameter of cold helium flow channels	8.0 cm	n/a	n/a	n/a
Radial location of cold helium flow channels	144.6 cm	n/a	n/a	n/a
Height of cold helium flow channels	505.0 cm	n/a	n/a	n/a
Diameter of control rod and irradiation channels	13.0 cm	n/a	n/a	n/a
Height of control rod and irradiation channels	450.0 cm	n/a	n/a	n/a
Radial location of control rod and irradiation channels	102.1 cm	n/a	n/a	n/a
Diameter of round part of KLAK channels	6.0 cm	n/a	n/a	n/a
Width of oval part of KLAK channels	6.0 cm	n/a	n/a	n/a
Length (in plane of cross section) of oval part of KLAK channels	16.0 cm	n/a	n/a	n/a
Diameter of hot gas duct	30.0 cm	n/a	n/a	n/a
Elevation of hot gas duct axis	480.0 cm	n/a	n/a	n/a
Length of hot gas duct	100.0 cm	n/a	n/a	n/a
Radius of fuel discharge tube	25.0 cm	n/a	n/a	n/a
Length of fuel discharge tube	221.236 cm	n/a	n/a	n/a
Diameter of fuel pebble	6.0 cm	5.98-6.0	5.98-6.0	n/a
Diameter of kernel	0.5 mm	0.5	0.501	0.025 des, 0.0102 exp
Thickness of buffer layer	0.09 mm	0.09	0.0902	0.018 des, 0.0044 exp
Thickness of IPyC layer	0.04 mm	0.03-0.05	0.0368-0.0424	n/a
Thickness of SiC layer	0.035 mm	0.031-0.039	0.0324-0.0376	n/a
Thickness of OPyC layer	0.04 mm	0.03-0.05	0.039-0.045	n/a
Packing fraction	0.61	n/a	n/a	n/a

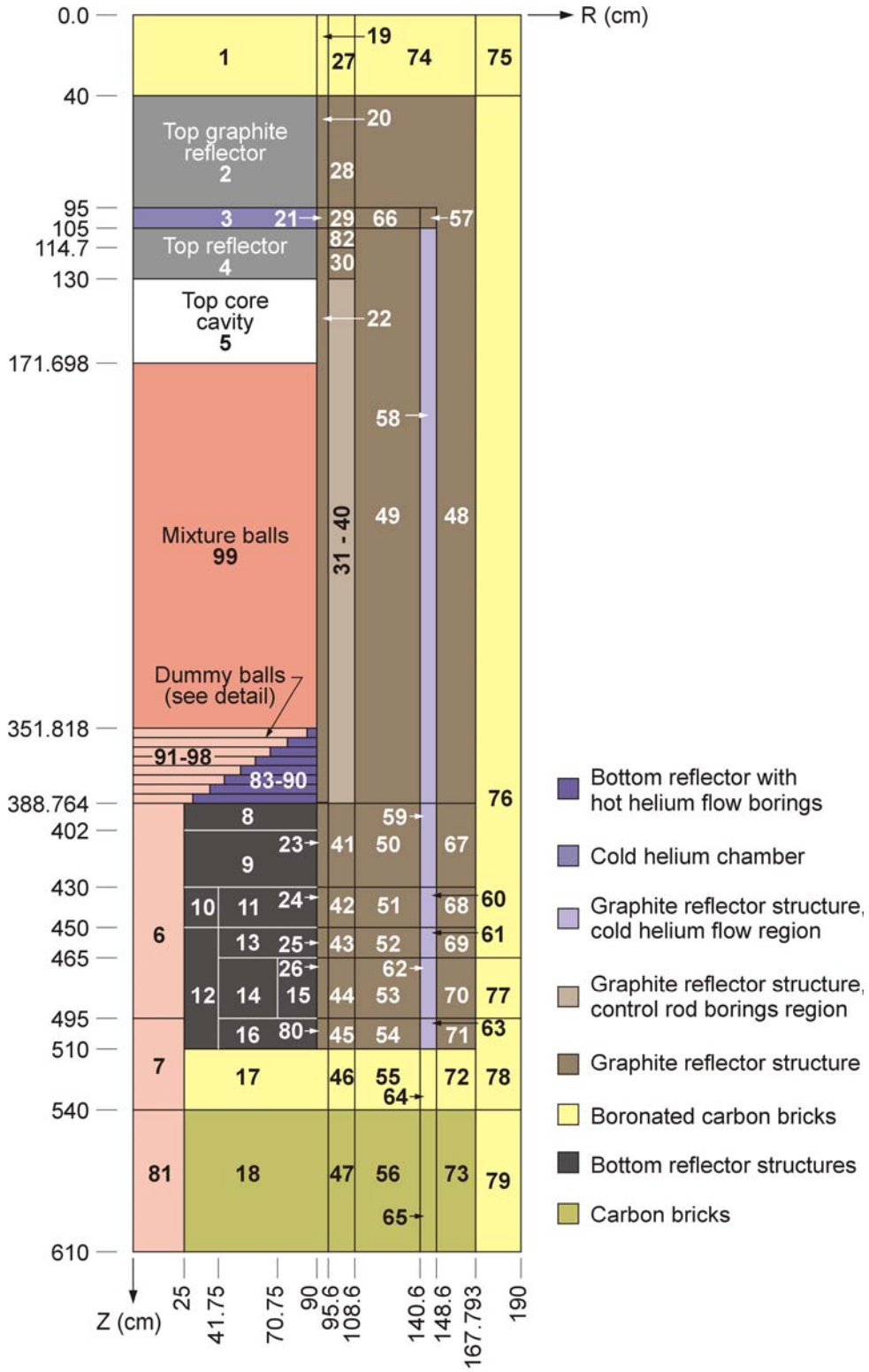

Figure 3(a). Zones of HTR-10 for modeling (dimensions are in cm)

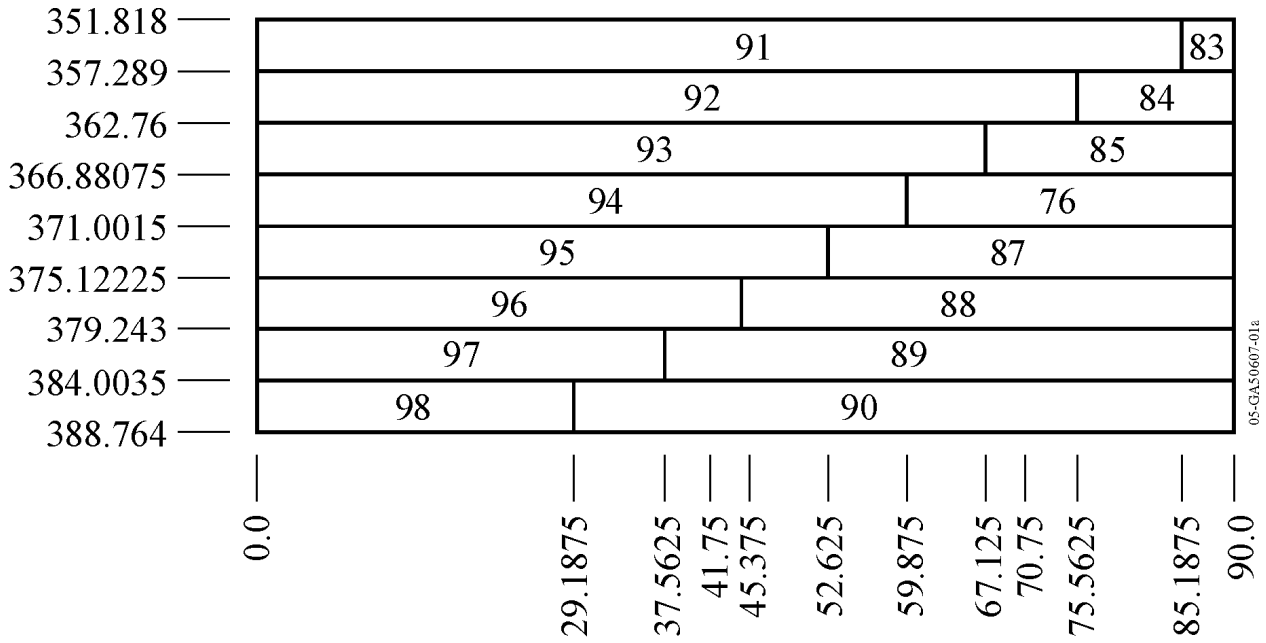

Figure 3(b). Detail in conus region (dimensions are in cm)

Figure 4 shows a horizontal cross section at an elevation within the core, displaying the borings for coolant flow channels, control rod and experiment channels, and emergency shutdown absorber ball channels. Figure 4 also shows the cross section of the emergency shutdown absorber ball channels in the section next to the core (above and below the core region, these channels are circular in cross section).

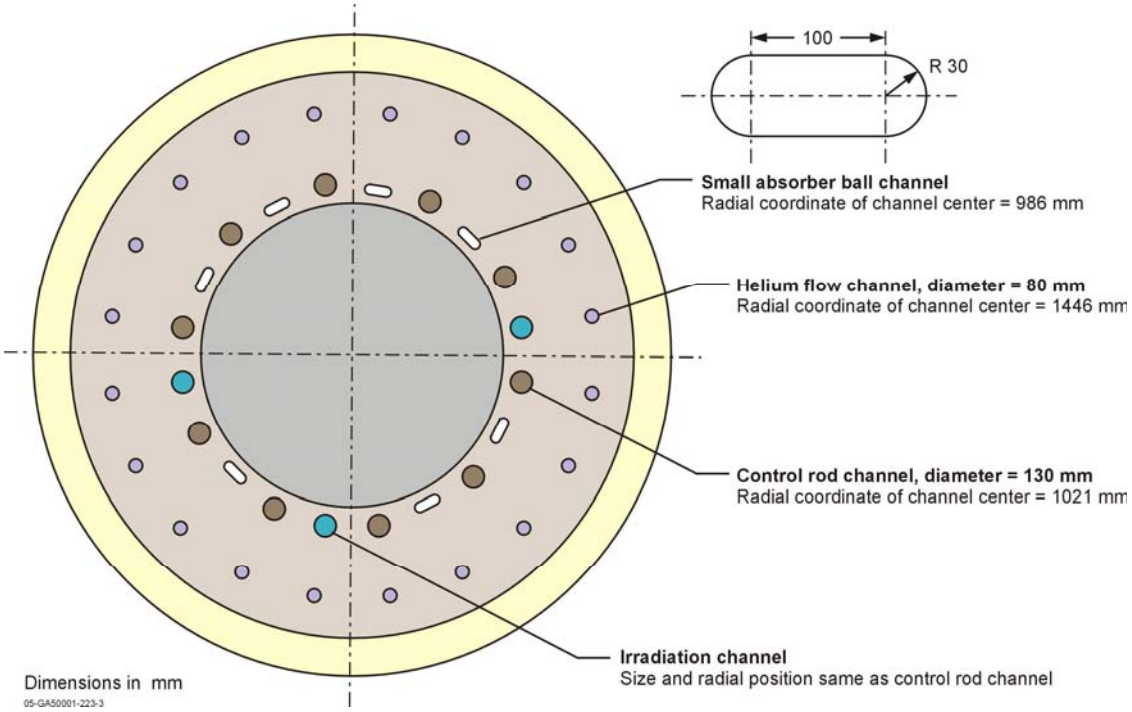

Figure 4. Cross section of reactor in core region

1.1.3 Description of Material Data

The nominal data for the fuel and dummy ball materials, in the actual as-built configuration, are given in Table 4. The material data for the reflector region are given in Table 5 for the zones shown in Figure 3.

The only materials specified in Table 5 are carbon and natural boron. The relative boron fraction varies among reflector zones, especially where highly boronated graphite is used to absorb neutrons near the periphery of the reflector. The graphite density also varies, because many of the zones have voids for various purposes. Since the control rods were withdrawn in the initial criticality experiment, and since no emergency neutron absorber balls had been introduced into the reflector, all the voids were assumed to be filled with air.

Although the HTR-10 is cooled by helium in operation, in the initial criticality experiment the voids in the reactor were filled with "moist" air at a total pressure of 0.1013 MPa and a temperature of 15 °C. The word "moist," which was used by the HTR-10 modeling group, is taken to mean saturated, as the water vapor density specified at the nominal temperature of 27 °C (see Section 1.1.4) is in fact the saturation density.

Table 4. Nominal material properties of fuel and dummy pebbles as built (from Reference 1)

Density of graphite in matrix and outer shell	1.73 g/cm3
Heavy metal (uranium) loading (weight) per ball	5.0 g
Enrichment of 235U (weight)	17 %
Equivalent natural boron content of impurities in uranium	4 ppm
Equivalent natural boron content of impurities in graphite	1.3 ppm
Volumetric filling fraction of balls in the core	0.61
UO2 density(g/cm3)	10.4
Coating layer materials (starting from kernel)	Buffer/PyC/SiC/PyC
Coating layer density(g/cm3)	1.1/1.9/3.18/1.9
Density of graphite in dummy balls	1.84 g/cm3
Equivalent natural boron content of impurities in graphite in dummy balls	0.125 ppm

Table 6 specifies the compositions of all the components in the reactor. Tolerance limits and observed ranges are shown where they are known. The nominal compositions are taken from Reference 1, and the uncertainties are taken from Reference 2. As noted above for the dimensions, Reference 2 presents data obtained by 1997, so it might not reflect tolerances or observations in the year of the experiment, but it contains the only information found on the tolerance specifications for the HTR-10.

1.1.4 Temperature Information

The initial criticality experiment was run with a clean cold core. In the benchmark specifications provided in advance of the experiment, the temperature was given as 20 °C, and the composition of the air actually occupying the void spaces in the reactor was specified at 27 °C, but the actual temperature on the day of the experiment was 15 °C . The actual temperature, 15 °C , is used in this evaluation.

1.1.5 Additional Information Relevant to Critical and Subcritical Measurements

No additional information is applicable.

Table 5. Compositions of zones shown in Figure 3 (from Reference 1, with revisions)

No. of zone	Carbon density (a/b-cm)	Natural boron density (a/b-cm)	Remarks
83-90	0.851047E-01	0.456926E-06	Bottom reflector with hot helium flow borings
1	0.729410E-01	0.329811E-02	Boronated carbon bricks
2	0.851462E-01	0.457148E-06	Top graphite reflector
3	0.145350E-01	0.780384E-07	Cold helium chamber
4	0.802916E-01	0.431084E-06	Top reflector
5			Top core cavity
6,7,91-97	0.572501E-01	0.277884E-08	Dummy balls, simplified as graphite of lower density
8	0.781408E-01	0.419537E-06	Bottom reflector structures
9	0.823751E-01	0.442271E-06	Bottom reflector structures
10	0.843647E-01	0.298504E-03	Bottom reflector structures
11	0.817101E-01	0.156416E-03	Bottom reflector structures
12	0.850790E-01	0.209092E-03	Bottom reflector structures
13	0.819167E-01	0.358529E-04	Bottom reflector structures
14	0.541118E-01	0.577456E-04	Bottom reflector structures
15	0.332110E-01	0.178309E-06	Bottom reflector structures
16	0.881811E-01	0.358866E-04	Bottom reflector structures
17,55,72, 74,75,76, 78,79	0.765984E-01	0.346349E-02	Boronated carbon bricks
18,56,73	0.797184E-01	0.000000E+00	Carbon bricks
19	0.761157E-01	0.344166E-02	Boronated carbon bricks
20	0.878374E-01	0.471597E-06	Graphite reflector structure
21	0.579696E-01	0.311238E-06	Graphite reflector structure
22,23,25, 49, 50,52,54, 66, 67,69,71, 80	0.882418E-01	0.473769E-06	Graphite reflector structure
24,51,68	0.879541E-01	0.168369E-03	Graphite reflector structure
26	0.846754E-01	0.454621E-06	Graphite reflector structure
27	0.589319E-01	0.266468E-02	Boronated carbon bricks
28,82	0.678899E-01	1.400000E-05	Graphite reflector structure
29	0.403794E-01	1.400000E-05	Graphite reflector structure
30,41	0.678899E-01	0.364500E-06	Graphite reflector structure
31-40	0.634459E-01	0.340640E-06	Graphite reflector, control rod borings region
42	0.676758E-01	0.125331E-03	Graphite reflector structure
43,45	0.861476E-01	0.462525E-06	Graphite reflector structure
44	0.829066E-01	0.445124E-06	Graphite reflector structure
46	0.747805E-01	0.338129E-02	Boronated carbon bricks
47	0.778265E-01	0.000000E+00	Carbon bricks
48	0.582699E-01	0.312850E-06	Graphite reflector structure
53	0.855860E-01	0.459510E-06	Graphite reflector structure
57	0.728262E-01	0.391003E-06	Graphite reflector structure
58,59,61, 63	0.760368E-01	0.408240E-06	Graphite reflector, cold helium flow region
60	0.757889E-01	0.145082E-03	Graphite reflector, cold helium flow region
62	0.737484E-01	0.395954E-06	Graphite reflector, cold helium flow region
64	0.660039E-01	0.298444E-02	Boronated carbon bricks
65	0.686924E-01	0.000000E+00	Carbon bricks
70	0.861500E-01	0.462538E-06	Graphite reflector structure
77	0.749927E-01	0.339088E-02	Boronated carbon bricks
81	0.847872E-01	0.000000E+00	Dummy balls, but artificially taken as carbon bricks

Table 6. Nominal values and variations in compositions

Item	Nominal Value	Design Tolerances	Observed Range	Standard Deviation
Uranium fuel loading (g/fuel pebble)	5.0 g	4.9-5.1	4.95-5.05	n/a
Density of graphite matrix in fuel pebble	1.73 g/cm3	1.73-1.77	1.73	n/a
Total ash in fuel element	0	≤300.0 ppm	130-190	n/a
Lithium in fuel element	0	≤0.3 ppm	0.007-0.023	n/a
Boron in fuel element	1.3 ppm	≤3.0 ppm	0.15	n/a
Density of graphite matrix in reflector	1.76 g/cm3	n/a	n/a	n/a
Density of boron in natural graphite reflector elements	4.8366 ppm	n/a	n/a	n/a
Ratio of oxygen to uranium in kernel	2	<2.01	n/a	n/a
Density of kernel	10.4 g/cm3	>10.4	10.83	n/a
Density of buffer layer	1.1 g/cm3	≤1.1	1.02	0.03 exp
Density of IPyC layer	1.9 g/cm3	1.8-2.0	1.80-1.92	n/a
Density of SiC layer	3.18 g/cm3	≥3.18	3.19-3.23	n/a
Density of OPyC layer	1.9 g/cm3	1.8-2.0	1.85-1.89	n/a
Composition of coolant	1.149e-3 g/cm3	n/a	n/a	n/a
Moisture content of coolant	2.57E-5 g/cm3	n/a	n/a	n/a

1.2 Description of Buckling and Extrapolation Length Measurements

No buckling or extrapolation length measurements were reported.

1.3 Description of Spectral Characteristics Measurements

No spectral characteristics were measured.

1.4 Description of Reactivity Effects Measurements

With a slight excess reactivity (i.e., at a total loading of 17,000 pebbles, or 110 more than the critical count), a control rod worth calibration experiment was carried out. One "typical" control rod was inserted a distance of 223 cm from its withdrawn position. The integral worth of the control rod was measured to be 1.4693%.

1.5 Description of Reactivity Coefficient Measurements

No reactivity coefficient measurements were made.

1.6 Description of Kinetics Measurements

No kinetics parameters were measured.

1.7 Description of Reaction-Rate Distribution Measurements

No reaction-rate distribution measurements were made.

1.8 Description of Power Distribution Measurements

No power distribution measurements were made.

1.9 Description of Isotopic Measurements

No isotopic measurements were made.

1.10 Description of Other Miscellaneous Types of Measurements

No other measurements have been reported.

2.0 EVALUATION OF EXPERIMENTAL DATA

The overall uncertainty in a calculated parameter that is a function of multiple input parameters is given by[1]

$$u_c^2(k_{eff}) = \sum_{i=1}^{N} (\Delta k_i)^2 + 2\sum_{i=1}^{N-1} \sum_{j=i+1}^{N} (\Delta k_i)(\Delta k_j) r_{i,j} \quad (1)$$

In Equation 1, Δk_i is the change in k_{eff} when parameter i is changed by the increment u_i, the standard uncertainty in the parameter, and $r_{i,j}$ is the correlation coefficient for parameters i and j.

Data on dimensions and materials are given in Table 4 (Section 1.1.2). Most of the data are given only as nominal values, with no information provided about tolerances, observed variations, or standard deviations. Where standard deviations are available, they are used for calculating the u_i. Where observed ranges are given, but not standard deviations, the limiting values of the observed ranges are usually applied, and plausible distribution functions are assumed for finding the u_i. Where only tolerances are given, their limiting values are used, along with plausible distribution functions. Where no guidance is given on the variability of a parameter, conservative engineering judgment is used. All uncertainties are adjusted to values of 1σ.

One category of unknown dimensional uncertainties includes the dimensions of the graphite blocks from which the reflector is constructed. In typical milling operations, tolerances on the order of tenths of millimeters are common. Cumulative uncertainties from stacking a set of ten or so blocks milled with such tolerances would be on the order of millimeters or less. For conservatism, a tolerance of ±1 cm is usually assumed for dimensions specifying the positioning of graphite reflector elements. Because borings have to line up much more precisely than that, a tolerance of 0.25 cm is usually assumed for the locations and radii of the various channels in the core.

Usually, no information is given about the distribution function of the deviation of a parameter from its nominal value. In most cases, it is assumed for convenience that the most relevant quantity is uniformly distributed. For example, if the change in k_{eff} from its nominal value is proportional to the change in the volume of a spatial region, then it is assumed that the deviation of the volume of that region from its nominal value is uniformly distributed.

The following subsections discuss the calculation of the uncertainties in the parameters listed in Table 4. The values of k_{eff} are computed in the as-run critical configuration and in the configuration with each parameter assigned its maximum variation (or its standard deviation

(1) " ICSBEP Guide to the Expression of Uncertainties," Larry G. Blackwood, Independent Reviewer, Revision 1, September 30, 2004, p. 29. This guide has not been published, but it is available to anyone involved in the IRPhEP.

when available), one parameter at a time. The bases for the choices of the parameter values are discussed. Only a few parameters are important enough that reasonable variations in them produce relatively large variations in k_{eff}; these parameters are discussed at greater length.

The value of k_{eff} computed for a given configuration depends on the microscopic cross sections used in the calculation. The calculated microscopic cross sections are somewhat sensitive to the fast and thermal buckling values used in the input to COMBINE, the cross section processing code[1] used in this evalution. The buckling values were found by a buckling search, as explained in subsection 3.1.1. In most cases, variations in the problem specifications were small enough that the same cross sections were used for both the critical baseline configuration and the perturbed configuration. However, in some cases, new cross sections were calculated for a perturbed case. The baseline value of k_{eff} is 1.03257.

The baseline value of k_{eff} computed for this evaluation is farther from 1.0 than one would like to see. PEBBED,[2] the code used to calculate k_{eff}, has been validated extensively[3] but its results are naturally dependent on the quality of the cross sections supplied to it. Calculation of cross sections in graphite systems presents problems that have not yet been resolved. Another possible source of inaccuracy is the shape of the upper surface of the core. Pebbles fall onto the upper surface at discrete drop points, where mounds build up, and they roll down a mound until they lodge more or less randomly on the surface. PEBBED assumes a planar upper core surface, like all the benchmark models reported in Reference 1. The error introduced by this assumption is not known. However, it introduces a constant bias in the results, and the uncertainty analysis should be unaffected by this bias.

Another possible source of inaccuracy in the PEBBED results is the use of only two spectral zones in the model – one in the core, and the other in the reflector. This might be inadequate, even in the HTR-10 initial startup core, which is uniform in composition. Again, however, this representation introduces in the results a constant bias that will not affect the uncertainties calculated when dimensional or compositional parameters are varied.

---

(1) Robert A. Grimesey, David W. Nigg, and Richard L. Curtis, *COMBINE/PC – A Portable ENDF/B Version 5 Neutron Spectrum and Cross-Section Generation Program*, EGG-2589, Rev. 1, Idaho National Engineering Laboratory, February 1991.

(2) W. K. Terry, H. D. Gougar, and A. M. Ougouag, "Direct Deterministic Method for Neutronics Analysis and Computation of Asymptotic Burnup Distribution in a Recirculating Pebble-Bed Reactor," Annals of Nuclear Energy 29 (2002), pp. 1345-1364.

(3) Hans D. Gougar, Abderrafi M. Ougouag, and William K. Terry, "Validation of the Neutronic Solver within the PEBBED Code for Pebble Bed Reactor Design," proc. *Mathematics and Computation, Supercomputing, Reactor Physics and Nuclear and Biological Applications,* Palais des Papes, Avignon, France, September 12-15, 2005, American Nuclear Society, LaGrange Park, IL (2005)

Another minor source of inaccuracy in the PEBBED results is the assumption that the core density is uniform. Of course, the pebble packing fraction is only about 61%, so on the scale of a pebble diameter the density is highly nonuniform, but on the scale of the core dimensions, this nonuniformity is not expected to make much difference. However, spheres in a container are not distributed uniformly throughout. It has been observed experimentally[(1)] that the packing fraction varies from zero at the edges through several damped oscillations to approach an asymptotic value of about 61% over a distance of about five sphere diameters. The effects of these inhomogeneities have been studied for a simple hypothetical PBR reactor configuration.[(2)] It was found that the difference in the calculated value of k_{eff} was about $5x10^{-4}$ for that reactor. The packing fraction itself is uncertain, but the uncertainty in this parameter is addressed in the analysis.

For perspective, the results of the international benchmark collaboration are noted, as given in Reference 1. The objective of the initial criticality benchmark was to predict the initial critical core height. The measured height was 123.06 cm, and the assumed temperature for the predictions was 20 °C. Predictions by various groups ranged from 107 cm to 137.3 cm. These values range from -13% to +12% of the core height. It is reported in subsection 2.1.1 below that a difference of 0.1% in the core height produces a difference of $3.7x10^{-4}$ in k_{eff}. If the relationship between the difference in k_{eff} and the difference in core height were linear over the entire range of core heights, the errors in k_{eff} would vary from -0.048 to +0.044, corresponding to a range in k_{eff} of 0.952 to 1.044. Computation of k_{eff} in PBRs is evidently not straightforward, and considerable research seems needed before accuracy is routinely obtained comparable to that in computations for light water reactors.

2.1 Evaluation of Critical Configuration Data

The following subsections contain evaluations of the critical configuration measurements described in Section 1.1. In many cases, the assumptions on the uncertainties in experimental parameters are very crude. However, the only important parameters are those whose uncertainties lead to uncertainties of more than 10^{-3} in k_{eff}. When reasonable and conservative assumptions lead to smaller uncertainties than that in k_{eff}, little is to be gained by trying to be more precise.

In all cases where tolerances or observed variations apply to large numbers of objects (pebbles

(1) R. F. Benenati and C. B. Brosilow, "Void Fraction Distribution in Beds of Spheres," *A. I. Ch. E. Journal* **8**, No. 3, pp. 359-361 (1962).

(2) W. K. Terry, A. M. Ougouag, Farzad Rahnema, and Michael Scott McKinley, "Effects of spatial variations in packing fraction on reactor physics parameters in pebble-bed reactors," American Nuclear Society Mathematics & Computation Division Conference, Gatlinburg, Tennessee, April 6-11, 2003.

and fuel particles or portions thereof), both systematic errors (applying to all the objects equally) and random errors (different from one pebble to the next) will occur. For the fuel particles and their subregions especially, the uncertainties from the random errors are extremely small (the tolerance limit for the random error divided by the square root of the number of fuel particles, √(4751x16,890) = 8957.9 (see Appendix B)). For errors in properties of pebbles, the uncertainty in the random component is equal to the tolerance limit for the random component divided by the square root of the number of pebbles, or 129.96. In all cases, division by such large numbers would make the random component of the uncertainty negligible. However, since nothing is known about how the errors are divided between the systematic and random components, it is assumed throughout that the errors are all systematic. This assumption provides the analysis with a large degree of conservatism.

When a variable x is judged to be distributed uniformly between the bounding values μ and $\mu+a$, the standard deviation in x can be shown to be $a/\sqrt{3}$.[(1)] (The reference actually proves the claim for a uniform distribution from $\mu-a$ to $\mu+a$, but the extension of the proof to the half-interval is trivial.) Then the standard deviation of a linear function $f(x)$ is $f(a/\sqrt{3})$. This observation is used repeatedly in the following analysis.

2.1.1 Core Height and Core Diameter

The core height is a calculated parameter, based on the number of balls contained in the core. As discussed above, the upper core surface is actually a mound, but it is modeled as a plane at an elevation consistent with the core volume and a cylindrical core shape. The total number of balls (fuel and dummy) in the cylindrical core region at criticality was given as 16,890, and no information was given on the accuracy of the count. The core height was computed from the number of balls and the nominal core diameter at an assumed packing fraction of 0.61.

The number of pebbles in the core is

$$N_p = \frac{\pi f_p R_c^2 H_c}{V_p} \quad , \tag{2}$$

where f_p =packing fraction,
R_c = core radius,
H_c = core height,
and V_p = pebble volume.

Then, in part, k_{eff} is a function of the packing fraction, core radius, core height, and pebble volume. The dependencies of k_{eff} on pebble volume and packing fraction are treated in

(1) " ICSBEP Guide to the Expression of Uncertainties," Larry G. Blackwood, Independent Reviewer, Revision 1, September 30, 2004, p. 29. This guide has not been published, but it is available to anyone involved in the IRPhEP.

subsequent subsections. In this subsection, pebble volume and packing fraction are held constant. It is convenient to treat core radius and core height together; it is reasonable to treat them as independent (uncorrelated) variables.

No estimate is given on the uncertainty in the number of balls in the core, but engineering judgment suggests that a counting accuracy of less than 1% would be very poor, while an accuracy of 0.1% (at one standard deviation) might be acceptable. The latter figure corresponds to a miscount of about 17 balls in the core. PEBBED calculations (based on changes of 1 cm in radius and height) show that a change in the core radius leads to a change in k_{eff} of 1.10643×10^{-5} per ball, while a change in core height leads to a change in k_{eff} of 2.16393×10^{-5} per ball. (This difference in sensitivity is due to the relatively short and wide configuration of the core at initial criticality). Then for a miscount of 17 balls,

$u_{core\ radius} = 1.9 \times 10^{-4}$
and
$u_{core\ height} = 3.7 \times 10^{-4}$.

2.1.2 Height of Core Cavity

This parameter is the height of the cavity in which the core resides, which includes the void space above the core, not the height of the core itself. The effect on k_{eff} of variations in this parameter is assessed by raising the datum plane at the top of the core cavity. No other computational cells are affected by this change. No guidance is given on the possible variation in core cavity height, but this parameter depends on the precision with which the graphite components of the reflector are milled. As noted above, a very conservative value of 1 cm is assumed for most graphite dimensional uncertainties. If the top of the core cavity is raised by 1 cm, k_{eff} changes by -4.2×10^{-4}. For lack of specific knowledge about how errors in core cavity height might be distributed, it is conservatively assumed that the distribution is uniform. Then the standard deviation in core height errors and the resulting change in k_{eff} are the limiting value divided by $\sqrt{3}$ (cf. Footnote (a)):

$u_{core\ cavity} = -2.4 \times 10^{-4}$.

2.1.3 Height of Conus

An uncertainty in the height of the conus is represented by moving the datum plane at the top of the conus upwards by 2.7355 cm, an increment that fits conveniently with the PEBBED nodalization, and by moving the datum plane at the top of the core by an equal amount. Thus, the active core height does not change. The shift roughly amounts to one pebble radius, which corresponds to a miscount of about 375 pebbles, an unlikely amount. For this assumed uncertainty, the change in k_{eff} is found to be 1.05×10^{-3}. Conservatively assuming a uniform distribution function for errors in conus height, one divides this number by $\sqrt{3}$ to find (to the

nearest significant figure)

$u_{conus} = 6.1 \times 10^{-4}$.

2.1.4 Dimensions of Graphite Blocks

As discussed in Section 2.0, tolerances of about 0.1 mm are assumed for milling the graphite blocks. Such tolerances appear reasonable in view of the necessity of coolant, control rod, and emergency absorber ball channels to line up. Except in the outer periphery of the reflector, where boronated carbon bricks are used to reduce neutron leakage into the surroundings, the only differences among adjacent blocks are in their void fraction; uncertainties in void fraction are accounted for below where the sizes and locations of the different borings are varied. Uncertainties in the inner and outer reflector diameters and the inner and outer reflector axial dimensions are also treated in other subsections. The importance of neutrons is low in the outer periphery. Therefore, it is not necessary to analyze the effects of uncertainties in the internal boundaries between reflector blocks.

2.1.5 Outer Diameter of Graphite Reflector

The outer diameter of the reflector could differ from the nominal value by an accumulation of off-nominal radial dimensions in graphite blocks at several radial locations or by off-nominal radial dimensions at a single radial location. Two cases of the latter possibility were explored. First, the outermost zone was increased 1 cm in radius; this led to an increase in k_{eff} of 1.8×10^{-4}. Second, with the outermost zone again at its nominal thickness, the next-to-outermost zone was increased 1 cm in radius; this led to a decrease in k_{eff} of 1.4×10^{-4}.

The outermost zone consists of boronated carbon bricks, installed for the purpose of capturing neutrons that would otherwise escape into the surrounding pressure vessel (which was not represented in the model provided in Reference 1 by the Chinese research group). Even though boron has a high absorption cross section for thermal neutrons, increasing the thickness of the boronated carbon bricks provides more scattering sites from which neutrons can be scattered back towards the core. In other words, nothing is as good an absorber as a vacuum boundary condition, so replacing vacuum with anything increases k_{eff}. However, increasing the thickness of the region inside the boronated graphite layer is found to decrease k_{eff}. It is surmised that this additional layer of low-boron graphite softens the neutron energy spectrum slightly, which increases the absorption of neutrons in the boronated carbon bricks and decreases the number of neutrons that can be reflected back into the core.

The larger effect is taken as the uncertainty in k_{eff} resulting from differences in the reflector outer diameter from the nominal value. The change in k_{eff} is proportional to the change in the cross-sectional area of the outermost zone. If the error in the cross-sectional area is uniformly distributed, a reasonable assumption, then the uncertainty in k_{eff} associated with uncertainty in reflector outside diameter is $1.8 \times 10^{-4}/\sqrt{3}$, or (to the nearest significant figure)

$u_{refl\ O.D.} = 1.0\text{x}10^{-4}$.

2.1.6 Height of Graphite Reflector

In this case, because of the large height of the reflector, a greater uncertainty was assumed in the height: ±1%, which is a dimensional uncertainty of ±6.1 cm. Increasing the axial thickness of the first axial region increases k_{eff} by $1.0\text{x}10^{-5}$. Increasing the axial thickness of the last region by 6.1 cm causes no change in k_{eff}. Whatever distribution function applies, the error at the standard deviation is smaller, but when it is rounded to the nearest significant figure the value returns to $1\text{x}10^{-5}$.

$u_{refl\ ht} = 1\text{x}10^{-5}$.

2.1.7 Diameter of Cold Helium Flow Channels

The nominal diameter of the helium flow channels is 8.0 cm; tolerance information is not given. A very conservative tolerance of ±0.5 cm is assumed; more realistic tolerances would be of the order of a fraction of a millimeter.

The helium flow channels occupy portions of Regions 58-65 in Figure 3. From Table 2, one can infer the void fraction in each region (Regions 22, etc., have no voids) and the part of the void space taken by the flow channels in each region. Then a reduction in the flow channel diameter can be used to find the new void fraction and the new nuclide number densities in each region. It is found that a simultaneous reduction of 0.5 cm in all the flow channel diameters produces an increase in k_{eff} of $2\text{x}10^{-5}$. If the error in cross-sectional area is assumed to be distributed uniformly, then the uncertainty in k_{eff} is $2\text{x}10^{-5}/\sqrt{3}$, or, to the nearest significant figure,

$u_{He\ flow\ dia} = 1\text{x}10^{-5}$.

2.1.8 Radial Location of Cold Helium Flow Channels

The helium flow channels occupy the entire radial span of Regions 58-65; i.e., r = 140.6-148.6 cm. (No tolerance information is given.) Therefore, the radial location of the channels can be adjusted by moving the inner and outer boundaries of these regions by equal amounts. The flow channels must line up well in axially adjacent blocks in order for the coolant to flow smoothly, so the tolerances in radial location must be quite small. For conservatism, it is assumed that the tolerance is 0.25 cm. An outward shift in the radial location of the flow channels produces a reduction of $4.0\text{x}10^{-5}$ in k_{eff}. If the error in radial location is distributed uniformly, then the uncertainty in k_{eff} is $4.0\text{x}10^{-5}/\sqrt{3}$, or, to the nearest significant figure,

$u_{He\ rad\ loc} = -2\text{x}10^{-5}$.

2.1.9 Height of Cold Helium Flow Channels

The cold helium flow channels extend to the bottom of the model in Figure 3. To change their height, one must extend them or contract them at the top. It was assumed for modeling convenience that the cold helium flow channels were extended through the entire axial span of region 57 of Figure 3, an increase of 10 cm. This is a very conservative assumption. This adjustment caused no change at all in k_{eff}.

$u_{He\ chan\ ht} = 0.0$

2.1.10 Diameter of Control Rod and Irradiation Channels

The control rod and irradiation channels are located at the same radial position and have the same diameter and axial extent. They occupy the entire radial span of Regions 27-31, 41, 42, and 82, or r = 95.6-108.6 cm. No tolerance range is given. The diameter is conservatively assumed to be 0.5 cm smaller than nominal. The same approach is applied as to the helium flow channels, discussed in Section 2.1.7 above. The change in k_{eff} is 6.1×10^{-4}, and the uncertainty is $6.1 \times 10^{-4}/\sqrt{3}$:

$u_{C\ R\ dia} = 3.5 \times 10^{-4}$.

2.1.11 Height of Control Rod and Irradiation Channels

The control rod and irradiation channels extend from the top of the core through Region 42 of Figure 3. The region below Region 31 is Region 43, which is 15 cm in height. Because neutrons are more important near the core than in the helium flow channel regions, it is excessively coarse to assume a perturbation in the height of the control rod and irradiation channels that extends the entire length of Region 43. It is assumed instead, still conservatively, that the perturbed channels extend 2 cm into Region 43. This perturbation does not change k_{eff}.

$u_{C\ R\ ht.} = 0.0$

2.1.12 Radial Location of Control Rod and Irradiation Channels

No tolerances are given on the location of the control rod and irradiation channels. If the inner and outer boundaries of the annulus containing these channels are moved outwards by 0.25 cm, the change in k_{eff} is 1.1×10^{-4}. Assuming a uniform error distribution in the radial location of the channels, one finds the uncertainty in k_{eff} to be

$u_{C\ R\ loc} = 6 \times 10^{-5}$.

2.1.13 Dimensions of KLAK Channels

The HTR-10 has two independent shutdown systems: the normal control rods and a supply of small spherical absorbers, often called "KLAK" from the German acronym for small absorber balls ("kleine aufsauger Kugeln"), that can be dropped into seven channels located in the same radial regions of the model as the control rod and irradiation channels. The KLAK channels run the entire length of the model. In the core and conus axial range, the channel cross sections are ovals 6 cm wide and 16 cm long, with the long sides oriented in the circumferential direction of the reactor. Above and below that axial range, the KLAK channels are cylindrical, with a diameter of 6 cm. No tolerance ranges are given.

The channels occupy a 6 cm radial zone in model regions 13 cm in radial extent. The KLAK channels can move in a range of 7 cm radially in these regions without changing the region densities. Such large perturbations in the KLAK channel locations are implausible. Therefore, the effects of radial mislocations of the KLAK channels are not modeled. However, the effects of perturbations in the size of the channels indicate that the effects of such mislocations are probably very small.

For the KLAK channels, an uncertainty of 10% (in standard deviation) was assumed in the cross-sectional area for all regions. This corresponds to about 5% in linear dimensions ($\sqrt{1.1}$ = 1.04881), or about 1.5 mm in radius in the cylindrical sections and 8 mm in the long direction in the oval section. The uncertainties in k_{eff} were computed from such increases in the sizes of the three sections of the KLAK channels.

Upper cylindrical section: $u_{KLAK\ upper} = 0.0$

Oval section : $u_{KLAK\ middle} = -2.8 \times 10^{-4}$.

Lower cylindrical section: $u_{KLAK\ lower} = 0.0$.

2.1.14 Dimensions of Hot Gas Duct

The hot gas duct extends from r=90 cm to the outer edge of the reflector, in regions 26, 44, 53, 62, 70, and 77 in an axial zone from z=465 cm to z=495 cm. The nominal diameter of the duct, 30 cm, spans this axial range. No tolerance ranges are given.

Because the duct is large, a large perturbation of 1 cm was assumed in the diameter. The same approach described above for the cold helium flow channels was applied to the duct diameter. The changed duct diameter had no effect on k_{eff}.

The effect of a perturbation in the length of the duct was examined by assuming the duct to extend through the radial extent of Region 15, which is adjacent to Region 26. This assumption

extends the length of the duct by 19.25 cm, which is completely unrealistic. However, the perturbation caused no change in k_{eff}, so more realistic perturbations would also have no effect.

A shift in the axial location of the duct could be accomplished by changing the locations of the datum planes at *z*=465 cm and *z*=495 cm, but this change would affect the nuclide number densities in other regions besides those containing the duct. An axial shift could also be represented by calculating perturbed nuclide number densities in regions adjacent to the nominal location of the duct, into which the duct would move in the perturbation, but this approach would alter the nuclide number densities throughout the adjacent regions, which would give distorted neutron flux distributions. Because of the lack of influence the other changes in duct dimensions have on k_{eff}, it is simply assumed that realistic shifts in hot gas duct axial position also have no effect.

$u_{hot\ gas\ duct} = 0.0$

2.1.15 Radius of Fuel Discharge Tube

The fuel discharge tube occupies regions 6, 7, and 81 in Figure 3. Its nominal radius is 25 cm; no tolerance range is given. The uncertainty in discharge tube radius is modeled by moving the radial boundary of Regions 6, 7, and 81 outwards by 0.25 cm. There is no effect on k_{eff}.

$u_{discharge\ radius} = 0.0$.

2.1.16 Height of Fuel Discharge Tube

The fuel discharge tube extends to the bottom of the model. The effect of increasing the height of the model has already been examined. A perturbation in the fuel discharge tube height is redundant.

$u_{discharge\ height} = 0.0$

2.1.17 Diameter of Fuel Pebble

The HTR-10 fuel pebble is a sphere 6 cm in diameter, consisting of an inner fuel zone 5 cm in diameter and an outer unfueled layer. The inner fuel zone consists of a graphite matrix containing an average of 8335 TRISO coated fuel particles. The outer layer contains only graphite. The core also contains dummy graphite balls, which are also 6 cm in diameter; the ratio of fuel balls to dummy balls is 57:43.

The tolerance range on fuel pebble diameter is 5.98-6.0 cm; this is also the observed range. The uncertainty in k_{eff} resulting from uncertainty in fuel pebble diameter is evaluated by reducing the pebble diameter to 5.98 cm.

There are several ways to do this, but the greatest changes in average nuclide densities in the core region are produced by keeping the diameter of the fuel zone constant and reducing the thickness of the outer graphite layer. For example, reducing the diameter of the fuel zone and keeping the outer graphite layer thickness constant would shrink the fuel zone volume almost in proportion to the shrinkage in total pebble volume; then the average nuclide densities in the core would be almost unaffected and k_{eff} would hardly change at all. The average densities are further changed by assuming that the dummy balls are also reduced to 5.98 cm in diameter. The result of making those changes is to decrease k_{eff} by 2.12×10^{-3}.

As noted in Section 2.1, the error within the tolerance range presumably comprises a systematic component and a random component. However, no information is available on how the error is apportioned between the systematic and random components. The most conservative approach is to assume that the error is all systematic. The uncertainty in the systematic component is equal to the tolerance limit for the systematic component divided by $\sqrt{3}$, assuming that the systematic error in volume is uniformly distributed (the change in k_{eff} is proportional to the volume change, not the linear change). Then the uncertainty in k_{eff} is $-2.12 \times 10^{-3}/\sqrt{3}$, or

$u_{FPdia} = -1.22 \times 10^{-3}$.

It merits comment that k_{eff} is reduced by packing more fuel balls, which each contain the same amount of fuel as the nominal pebbles, into the same volume of core. Evidently the HTR-10 is undermoderated, so that the loss of moderation caused by reducing the amount of graphite in the core overshadows the increase in the macroscopic fission cross section obtained by increasing the amount of fuel. A study of the effect of changing the relative amounts of fuel and moderator in PBRs has found that the usual formula of 5 cm for the fuel zone diameter and 6 cm for the fuel pebble diameter does not provide optimal moderation, at least for some fuel particle packing fractions.(1)

2.1.18 Diameter of Kernel

The nominal kernel diameter is 0.5 mm, and the measured standard deviation is 0.0102 mm. The 1-σ kernel is 6.2457% larger in volume than the nominal kernel. However, there is a tolerance in pebble fuel loading of 5.0±0.1 g/pebble. This is only a variation of ±2%. Therefore, if all of the kernels were allowed to reach their 1σ diameter, the limit on fuel loading would be exceeded. Hence, the limit on fuel loading (see Section 2.1.23) bounds the effects of uncertainties in the

(1) Abderrafi M. Ougouag, Hans D. Gougar, William K. Terry, Ramatsemela Mphahlele, and Kostadin N. Ivanov, "Optimal Moderation in the Pebble-Bed Reactor for Enhanced Passive Safety and Improved Fuel Utilization," proc. *PHYSOR 2004, The Physics of Fuel Cycles and Advanced Nuclear Systems: Global Developments,* American Nuclear Society, Chicago, IL, April 25-29, 2004.

fuel kernel diameter, and the fuel kernel diameter is not used in the uncertainty analysis.

2.1.19 Thickness of Buffer Layer

The buffer layer is a relatively porous layer of carbon immediately surrounding the kernel. Its porosity is intended to provide room for fission product gases without excessive pressure buildup. In the HTR-10 fuel, the buffer layer thickness is nominally 0.09 mm, and the experimentally observed standard deviation is 0.0044 mm. In the uncertainty analysis, it was assumed that all the buffer layers in the core were increased by one standard deviation from the nominal value, and that all the other layers in the fuel particles kept their original volumes. The new core average nuclide densities were computed, and k_{eff} was found to decline by $-3.0\text{x}10^{-5}$. It is assumed that the error in buffer volume is uniformly distributed; then the uncertainty in k_{eff} is $-3.0\text{x}10^{-5}/\sqrt{3}$, or, to the nearest significant figure,

$u_{buffer\ thickness} = -2\text{x}10^{-5}$.

The reason for the decrease in k_{eff} is that the expanded buffer layer displaces matrix material, since the diameter of the fuel zone is held constant. Then there is a decrease in carbon density in the core, which reduces moderation.

2.1.20 Thickness of IPyC Layer

Outside the buffer layer, the TRISO particle consists of three hard and dense layers that provide a miniature containment vessel for fission products. The first of these is the inner pyrolytic carbon (IPyC) layer. Its nominal thickness is 0.04 mm, its tolerance range is 0.03-0.05 mm, and its observed range of variation is 0.0368-0.0424 mm. For conservatism, it was assumed that all of the IPyC layers in the core were expanded to their maximum allowable thickness, while all the other layers retained their nominal volumes. The density of the pyrolytic carbon layers is greater than that of the matrix material, so expansion of the layers increases the carbon density in the core and enhances moderation. Therefore, k_{eff} increases slightly; the change is $3\text{x}10^{-5}$. If the volume error is uniformly distributed, then to the nearest significant figure,

$u_{IPyC\ thickness} = 2\text{x}10^{-5}$.

2.1.21 Thickness of SiC Layer

The second hard and dense layer outside of the buffer zone is the silicon carbide layer. This is the strongest layer in the fuel particle and the principal containment shell. It has a nominal thickness of 0.035 mm, a tolerance range of 0.031-0.039 mm, and an observed range of 0.0324-0.0376 mm. Standard deviations are not given. First, it was assumed that all of the SiC layers in the core were expanded to their maximum allowable thickness, while all the other layers retained their nominal volumes. This perturbation produced a decrease in k_{eff} of $-3.4\text{x}10^{-4}$.

In cases like the IPyC layer, where even perturbations up to the maximum tolerance value produce only very small changes in k_{eff}, it is both conservative and inconsequential to use the maximum allowable perturbation to compute the uncertainty in k_{eff}. However, when such a perturbation produces a larger change in k_{eff}, it is more reasonable to assume the maximum observed perturbation. The computed change in k_{eff} and the fractional volume change were applied were used to calculate

$$\frac{dk_{eff}}{d\bar{V}} = -2.70499x10^{-3}. \quad (3)$$

Then an increase of the SiC thickness to its maximum observed value gives a change in k_{eff} of $-2.2x10^{-4}$. If the change in SiC volume is assumed to be distributed uniformly, then

$u_{SiC\ thickness} = -1.3x10^{-4}$.

2.1.22 Thickness of OPyC Layer

The final hard and dense layer in the TRISO particle, and its outermost shell, is the outer pyrolytic carbon (OPyC) layer. This shell has a nominal thickness of 0.04 mm, a tolerance range of 0.03-0.05 mm, and an observed range of 0.039-0.045 mm. It was assumed that all the OPyC layers in the core were increased to their maximum allowable values while all the other layers retained their nominal volumes. This assumption led to an increase of $5x10^{-5}$ in k_{eff}. If the change in the OPyC volume is distributed uniformly,

$u_{OPyC\ thickness} = 3x10^{-5}$.

2.1.23 Uranium Fuel Loading

The nominal uranium loading in the HTR-10 fuel is 5 g per pebble. The tolerance range is 4.9-5.1 g, and the observed range is 4.95-5.05 g. The tolerance range was used to estimate the derivative

$$\frac{dk_{eff}}{d\bar{m}_U} = 0.179 \quad , \quad (4)$$

where $\bar{m}_U$ is the normalized uranium mass in the pebble.

The observed variation in $\bar{m}_U$ is ±1%, so the associated variation in k_{eff} is $1.79x10^{-3}$. If the deviation of the uranium loading from the nominal value is distributed uniformly within the observed range, the uncertainty in k_{eff} is

$1.79x10^{-3}/\sqrt{3}$, or

$u_{U\ loading} = 1.03x10^{-3}$.

2.1.24 Density of Graphite Matrix in Fuel Pebble

The density of the graphite matrix in the fuel pebble is nominally 1.73 g/cm^3. The tolerance range is 1.73-1.77 g/cm^3, and only the nominal value was observed. It is not plausible to assume that there is no uncertainty in the graphite density, but the observation of only one value suggests that a uniform distribution is not appropriate. For this case, a triangular distribution was assumed, with the mode (i.e., the most frequently observed value) equal to the nominal value and the distribution function declining to zero at the maximum tolerance value.

The variance in the triangular distribution is given by(1)

$$\sigma^2 = \frac{a^2 + b^2 + c^2 - ab - ac - bc}{18}, \tag{5}$$

where *a* and *b* are the limits of the interval on which the distribution function is defined, and *c* is the mode.

This formula was applied to the deviation of the graphite density from 1.73 g/cm^3, so that *a*=0, *b*=0.04, and *c*=0. Then $\sigma^2 = 8.88889x10^{-5}$ and $\sigma = 0.009428$. The uncertainty is found by computing k_{eff} at one standard deviation away from the nominal value. Thus, the value of the graphite matrix density at which k_{eff} is to be evaluated is 1.739428 g/cm^3. The boron content of the graphite matrix is assumed to remain at 1.3 ppm. The fuel matrix graphite is only one component of the carbon in the core region. All the other carbon components are assumed to be unaffected. When the new graphite and boron densities are used in PEBBED, the associated uncertainty in k_{eff} is found to be

$u_{fuel\ graphite\ density} = 1.13x10^{-3}$.

2.1.25 Total Ash in Fuel Element

The fuel specifications permit small amounts of unspecified impurities. Without knowing what they are, it is impossible to assess their effects quantitatively. However, it is not necessary to do so. The tolerance limits on the boron content of the fuel and reflector are actually limits on equivalent boron content, which includes the unspecified impurities.

---

(1) M. Evans, Nicholas Hastings, and Brian Peacock, *Statistical Distributions*, 3rd Edition, John Wiley and Sons, New York, 2000, pp. 187-188.

2.1.26 Lithium in Fuel Element

The nominal fuel element contains no lithium, but a trace amount of up to 0.3 ppm is permitted, and concentrations of 0.007-0.023 ppm are observed.

The maximum allowable amount of lithium was assumed, not only in the fuel elements but also in the dummy balls. A new cross section set was generated, and the revised multiplication constant was computed. The change in k_{eff} is 1.7×10^{-5}. The deviation of the lithium concentration from zero to the maximum allowable value is assumed to be uniform. Then the uncertainty in k_{eff} is $1.7 \times 10^{-5}/\sqrt{3}$, or

$u_{Li} = 1 \times 10^{-5}$.

2.1.27 Boron in Fuel Element

The nominal boron concentration in the fuel graphite is 1.3 ppm, while the tolerance limit is 3.0 ppm. The only observed value reported in Reference 2 for the boron in the fuel element graphite matrix is 0.15 ppm. As in the case of the fuel matrix graphite density, it requires judgment to choose a distribution function for the boron concentration. When, in contrast, the boron content in the dummy balls was found to differ substantially from the nominal value (the nominal value was 1.3 ppm, while the as-built value is reported as 0.125 ppm), the deviation was noted in the experiment report (Reference 1). One would expect that a deviation almost as great in the fuel element matrix boron would also have been reported. The nominal value is almost in the middle of the tolerance range. It is very conservative to assume a uniform distribution between the minimum and maximum values of 0 and 3.0 ppm, respectively, and to find k_{eff} at the maximum of 3.0 ppm.

When this value is used to adjust the boron concentration in all components of the fuel element except the kernels, for which a value of 4 ppm was used as reported in Reference 1, the change in k_{eff} from the baseline value is -7.43×10^{-3}. The uncertainty for a uniform distribution is $-7.43 \times 10^{-3}/\sqrt{3}$, or

$u_{fuel\ boron} = -4.29 \times 10^{-3}$.

2.1.28 Density of Graphite Matrix in Reflector

The nominal graphite density in the reflector material is 1.76 g/cm^3; no information is given on tolerances, observed ranges, or standard deviations. It is assumed that the total tolerance range is the same as for the graphite matrix in the fuel pebbles, i.e., 0.04 g/cm^3, but that the nominal value is centered in the range. So the assumed tolerance range becomes 1.76±0.02 g/cm^3. Furthermore, it is assumed that the deviation from the nominal value is distributed uniformly within this range. The boron content is assumed to vary in proportion to the carbon density.

With these assumptions, when k_{eff} is evaluated at a density of 1.78 g/cm^3, the change in k_{eff} becomes 1.09×10^{-3}, and the uncertainty is found to be $1.09 \times 10^{-3}\sqrt{3}$, or

$u_{reflector\ graphite} = 6.3 \times 10^{-4}$.

2.1.29 Density of Boron in Reflector Natural Graphite

Here, the boron is assumed to vary independently from the carbon density. The nominal boron concentration is 4.8366 ppm by weight; no information is given on tolerances, observed ranges, or standard deviations. This value applies to the natural graphite in the reflector, and not to boronated carbon bricks or other structures in which the boron concentration is elevated above the natural level.

The change in k_{eff} was calculated for a 10% deviation in boron density from the nominal value. The result was -5.00×10^{-3}. This is a very large effect, showing that k_{eff} is quite sensitive to the boron concentration, as one would expect. Accordingly, it is unlikely that a tolerance of ±10% would be considered acceptable. It is likely to be still conservative to assume a tolerance range of ±5%, which would approximately halve the change in k_{eff}. If the distribution function is uniform, the uncertainty is $-5.00 \times 10^{-3}/2\sqrt{3}$, or

$u_{reflector\ boron} = -1.44 \times 10^{-3}$.

2.1.30 Ratio of Oxygen to Uranium in Kernel

The nominal value is the stoichiometric ratio of 2.0; the tolerance limit is 2.01. It is assumed that the distribution is uniform from the nominal value to the limit. The multiplication factor is found to change by 1×10^{-5}, so that the uncertainty is $1 \times 10^{-5}/\sqrt{3}$, or, to the nearest significant figure,

$u_{O/U} = 1 \times 10^{-5}$.

2.1.31 Density of Kernel

The nominal kernel density is 10.4 g/cm^3, which is also the lower tolerance limit. The observed value is given in Reference 2 as 10.83 g/cm^3. The observed value is considerably higher than the nominal value, so new cross sections were computed for this uncertainty calculation. Then k_{eff} was found for a kernel density of 10.83 g/cm^3. The change in k_{eff} was found to be 5.48×10^{-3}.

This is a very large change in k_{eff}, but the difference in kernel density from the nominal value is

also quite large, namely 4.13%. There is a tolerance range on fuel loading per pebble, as discussed in subsection 2.1.24 above, of 4.9-5.1 g, or ±2%. Therefore, if all kernel densities were equal to the value reported in Reference 2, and if the number of kernels were unchanged, the pebble would exceed its tolerance on fuel loading. The fuel loading tolerance limit is bounding on the average kernel density, and the effects of variations in kernel density within the fuel loading tolerance limit are included in the uncertainty reported in subsection 2.1.23.

2.1.32 Density of Buffer Layer

The nominal value of the density of the buffer layer is 1.1 g/cm^3, the tolerance range is 0-1.1 g/cm^3, the observed value given in Reference 2 is 1.02 g/cm^3, and the standard deviation is 0.03 g/cm^3. The boron concentration is assumed to remain at 1.3 ppm. A deviation of 0.1 g/cm^3 was used to calculate $dk_{eff}/d\rho_{buffer}$,but the uncertainty was evaluated at the standard deviation; to the nearest significant figure, this is

$u_{buffer\ density} = -3\text{x}10^{-5}$.

2.1.33 Density of IPyC Layer

The nominal IPyC density is 1.9 g/cm^3, the tolerance range is 1.8-2.0 g/cm^3, and the observed range is 1.8-1.92 g/cm^3. No standard deviation is given. The change in k_{eff} from the nominal value was computed from the tolerance limit of 2.0 g/cm^3, with the boron concentration unchanged at 1.3 ppm. The change in k_{eff} was found to be $6\text{x}10^{-5}$; if the probability distribution is uniform, then to the nearest significant figure,

$u_{IPyC\ density} = 3\text{x}10^{-5}$.

2.1.34 Density of SiC Layer

The nominal SiC density is 3.18 g/cm^3, the tolerance range is ≥3.18 g/cm^3, the observed range is 3.19-3.23 g/cm^3, and no standard deviation is given. For conservatism, the change in k_{eff} was computed for the upper tolerance limit and found to be $-2\text{x}10^{-5}$. If the distribution in the range from 3.18-3.23 g/cm^3 is uniform, then to the nearest significant figure,

$u_{SiC\ density} = 1\text{x}10^{-5}$.

2.1.35 Density of OPyC Layer

The nominal OPyC density is 1.9 g/cm^3, the tolerance range is 1.8-2.0 g/cm^3, and the observed range is 1.85-1.89 g/cm^3. The derivative $dk_{eff}/d\rho_{OPyC}$ was calculated at the tolerance limit of 2.0 g/cm^3, but the distribution was assumed uniform between 1.85g/cm^3 and 1.9 g/cm^3 for simplicity

and conservatism; then the change in k_{eff} is -4.5×10^{-5} and the uncertainty is that value divided by $\sqrt{3}$; to the nearest significant figure, this is

$u_{OPyC\ density} = 3 \times 10^{-5}$.

2.1.36 Composition of Coolant

The coolant in actual reactor operation is helium, but in the initial criticality experiment the voids in the reactor were occupied by ambient air, which was specified as "moist" air at a total pressure of 0.1013 MPa and a temperature of 15 °C. The specified pressure of 0.1013 MPa is standard sea level atmospheric pressure, 29.92 in Hg. As mentioned in subsection 1.1.3, the term "moist" is taken to mean saturated. Therefore, the baseline composition is saturated air at 15 °C and 0.1013 MPa.

There are two potential causes of uncertainty in the specification of the coolant. First, the air was probably not fully saturated. Second, the air pressure was probably not standard sea level pressure. The second possibility is treated in the next subsection. A check of weather data in Beijing on the Internet shows a wide variability in the relative humidity, from low humidity (e.g., around 20%) to nearly saturated. The lowest possible value of relative humidity is zero. The change in k_{eff} from saturated air to totally dry air was found to be -3×10^{-5}. Assuming a uniform distribution between the extremes of humidity, one finds, to the nearest significant figure,

$u_{water\ vapor} = 2 \times 10^{-5}$.

2.1.37 Air Pressure

Standard sea level pressure is 29.92 in. Hg (0.1013 MPa). Sea level pressure typically varies about ±1 in. Hg. While larger variations are not uncommon, they represent more extreme weather than normal. Atmospheric pressure also varies with elevation above sea level; the elevation at Beijing is given on the Internet variously from 35 to 55 m. This is sufficiently close to sea level not to affect the standard atmospheric pressure significantly. A cursory search of the Internet failed to reveal a standard deviation for atmospheric pressure, so 1 in. Hg was taken as a conservative estimate. With the components of dry air made denser by a factor of 30.92/29.92, the change in k_{eff} was found to be -3.0×10^{-4}. This is a small change compared to some of the other uncertainties, and not worth trying to refine further.

$u_{air\ pressure} = -3.0 \times 10^{-4}$.

2.1.38 Boron in Kernels and Dummy Balls

Reference 1 gives the boron concentration in the kernels as 4 ppm and the boron concentration in

the dummy balls as 0.125 ppm. No information is given on tolerances, observed ranges, or standard deviations. No information was given on these boron concentrations in Reference 2.

It is implied that these concentrations are confidently known values. In the specifications for the international benchmark that was performed before the initial criticality experiment, the boron concentration in the dummy balls was given as 1.3 ppm, but Reference 1 states that the actual value was 0.125 ppm instead of the previously stated value of 1.3 ppm. This implies that the corrected value is known accurately. It seems unlikely that whatever tolerance range applies to this parameter is as large as those that apply to the reflector and fuel ball matrix graphite compositions. It is customary in such circumstances to assume an uncertainty of one-half the last digit, i.e, ±0.5x0.001=±0.0005, or ±0.4%. This is too small to merit analysis.

The argument to support confidence in the value of 4 ppm for the kernel boron concentration is less compelling, but in the absence of specific data on the variability of this parameter, the given value is taken as a measurement with the customary uncertainty of one-half the last digit: ±0.5x1=±0.5. This tolerance was applied to the kernel graphite, with a resulting change in k_{eff} of $-7x10^{-5}$. Assuming a uniform error distribution, one finds

$u_{kernel\ boron} = -4x10^{-5}$.

2.1.39 Packing Fraction

The average packing fraction is assumed to be 0.61, as has been observed experimentally.(1) But other packing fractions are theoretically possible, and a numerical study has shown that shifts in packing fraction, as might happen in an earthquake, can induce substantial changes (of the order of 1%) in k-effective.(1) Evidently an increase in packing fraction causes a reduction in leakage even though the total mass of the core remains constant.

The statistical variation in packing fraction in a bed of spheres is not known. It is unlikely that the packing fraction will exceed 0.64, which corresponds to the maximally random jammed state.(2) This is the condition where the pebbles are as closely packed as possible while remaining randomly arranged. Closer packing requires organized lattice structure.

In this analysis, it is assumed that the packing fraction varies uniformly in the range from 0.60-0.62. This assumption is believed to be conservative. When the inventory of core constituents

(1) A. M. Ougouag and W. K. Terry, "A Preliminary Study of the Effect of Shifts in Packing Fraction on k-effective in Pebble-Bed Reactors," American Nuclear Society Mathematics & Computation Division Conference, Salt Lake City, Utah, September 9-13, 2001.

(2) S. Torquato, T. M. Truskett, and P. G. Debenedetti, "Is Random Close Packing of Spheres Well Defined?" Phys. Rev. Lett. 84, p. 2064, 6 March 2000.

remains constant, a change in packing fraction entails a change in core height. This change is uncorrelated with the change analyzed in subsection 2.1.1, because there the change in core height was assumed to result from an inaccurate pebble count. The change in k_{eff} from an increase in packing fraction to 0.62 is found to be 3.3×10^{-3}, when the core height changes as needed to keep the core material inventories constant. For a uniform distribution, the corresponding uncertainty in k_{eff} is

$u_{packing\ fraction} = 1.90 \times 10^{-3}$.

2.1.40 Overall Uncertainty in k_{eff}

When Eq. 1 is applied to all the uncertainties calculated in subsections 2.1.1-2.1.39, assuming that all the uncertainties are uncorrelated (a reasonable and pragmatically necessary assumption), the result is

$u_{overall} = 5.41 \times 10^{-3}$, or about 0.5%.

This number was obtained by making consistently conservative assumptions on the variability of parameters on which k_{eff} may depend. The parameters that could have the largest effect are the various boron densities, the graphite matrix density, the fuel loading, and the pebble diameter. It is unlikely that any of the boron densities, on average, are as far from the nominal value as the tolerance range permits. Therefore, the initial criticality measurement in HTR-10 is judged to be an acceptable benchmark.

Table 7 summarizes the results of the uncertainty calculations.

Table 7. Individual and total uncertainties

Item	Uncertainty (u_i) (NA means not applicable – see text)
Core radius	1.9e-4
Core height	3.7e-4
Height of core cavity	2.4e-4
Height of conus	6.1e-4
Dimensions of graphite blocks	NA
Outer diameter of graphite reflector	1.0e-4
Height of graphite reflector	1e-5
Diameter of cold helium flow channels	1e-5
Radial location of cold helium flow channels	-2e-5
Height of cold helium flow channels	0
Diameter of control rod and irradiation channels	3.5e-4
Height of control rod and irradiation channels	0
Radial location of control rod and irradiation channels	6e-5
Diameter of KLAK channels (upper)	0
Dimensions of KLAK channels (middle)	-2.8e-4
Diameter of KLAK channels (lower)	0
Dimensions of hot gas duct	0
Radius of fuel discharge tube	0
Height of fuel discharge tube	0
Diameter of fuel pebble	1.22e-3
Diameter of kernel	NA
Thickness of buffer layer	-2e-5
Thickness of IPyC layer	2e-5
Thickness of SiC layer	-1.3e-4
Thickness of OPyC layer	3e-5
Uranium fuel loading	1.03e-3
Density of graphite matrix in fuel pebble	1.13e-3
Total ash in fuel element	NA
Lithium in fuel element	1e-5
Boron in fuel element	-4.29e-3
Density of graphite matrix in reflector	6.3e-4
Density of boron in reflector graphite	-1.44e-3
Ratio of O to U in kernel	1e-5
Density of kernel	NA
Density of buffer	-3e-5
Density of IPyC layer	3e-5
Density of SiC layer	1e-5
Density of OPyC layer	3e-5
Composition of coolant (saturated vs. dry air)	2e-5
Air pressure	-3e-4
Boron in kernels	-4e-5
Boron in dummy balls	NA
Packing fraction	1.9e-3
Total (root mean square)	5.41e-3

2.2 Evaluation of Buckling and Extrapolation Length Data

No buckling or extrapolation length measurements were made.

2.3 Evaluation of Spectral Characteristics Data

No spectral characteristics were measured.

2.4 Evaluation of Reactivity Effects Data

The control rod worth measurements have not yet been evaluated.

2.5 Evaluation of Reactivity Coefficient Data

No reactivity coefficients were measured.

2.6 Evaluation of Kinetics Measurements Data

No kinetics measurements were made.

2.7 Evaluation of Reaction-Rate Distributions

No reaction-rate measurements were made.

2.8 Evaluation of Power Distribution Data

No power distribution measurements were made.

2.9 Evaluation of Isotopic Measurements

No isotopic measurements were made.

2.10 Evaluation of Other Miscellaneous Types of Measurements

No other measurements were made.

3.0 BENCHMARK SPECIFICATIONS

3.1 Benchmark-Model Specifications for Critical and / or Subcritical Measurements

This section contains benchmark specifications for the critical configuration described in Section 1.1.

3.1.1 Description of the Calculational Model and Methodology

The geometry of the HTR-10 was divided into axisymmetric regions as shown in Figures 5 and 6. The definition of regions in Figure 5 is mostly as specified by the HTR-10 research group in its invitation to participants in its international benchmark project. The graphite and boron densities for the regions in Figure 5 were also supplied by the HTR-10 team in Reference 1; these are given in Table 8. The dimensions of components in the fuel and dummy pebbles are given in Table 9. The HTR-10 research group has access to the detailed design drawings and documents for their reactor; the data in these figures and tables are surely better than anything one could derive from publicly available documents. Thus, these data were used as the basis for the calculational model in this evaluation. For this evaluation, the INL code PEBBED[(1),(2)] was used to calculate k_{eff} for the nominal and perturbed configurations. PEBBED is a reactor physics and fuel management code developed by the Idaho National Laboratory (INL) specifically for PBRs. For compatibility with PEBBED, the numbering of some zones in the reflector, the conus, and the bottom reflector section with hot helium flow borings was changed slightly from the numbering assigned by the HTR-10 modeling group. Figure 5 shows the numbering used in this evaluation report. The only change that affects the fidelity of the model is the approximation of the straight, slanted surface of the conus by a series of stair-steps. This is a necessary approximation for the use of any code in cylindrical geometry; some participants in the pre-experiment benchmark program applied the same approach. The stair-steps are small, so that the effects of the approximation should be negligible; in any case, the approximation introduces a uniform bias in the results and will not corrupt the uncertainty calculation.

The PEBBED input deck for the nominal configuration is presented in Appendix A.

---

1 W. K. Terry, H. D. Gougar, and A. M. Ougouag, "Direct Deterministic Method for Neutronics Analysis and Computation of Asymptotic Burnup Distribution in a Recirculating Pebble-Bed Reactor," Annals of Nuclear Energy 29 (2002), pp. 1345-1364.

(2) H. D. Gougar, W. K. Terry, and A. M. Ougouag, *PEBBED V.4.3 Manual (DRAFT)*, Idaho National Engineering and Environmental Laboratory. This manual has not been published, but it will be provided to officially designated reviewers.

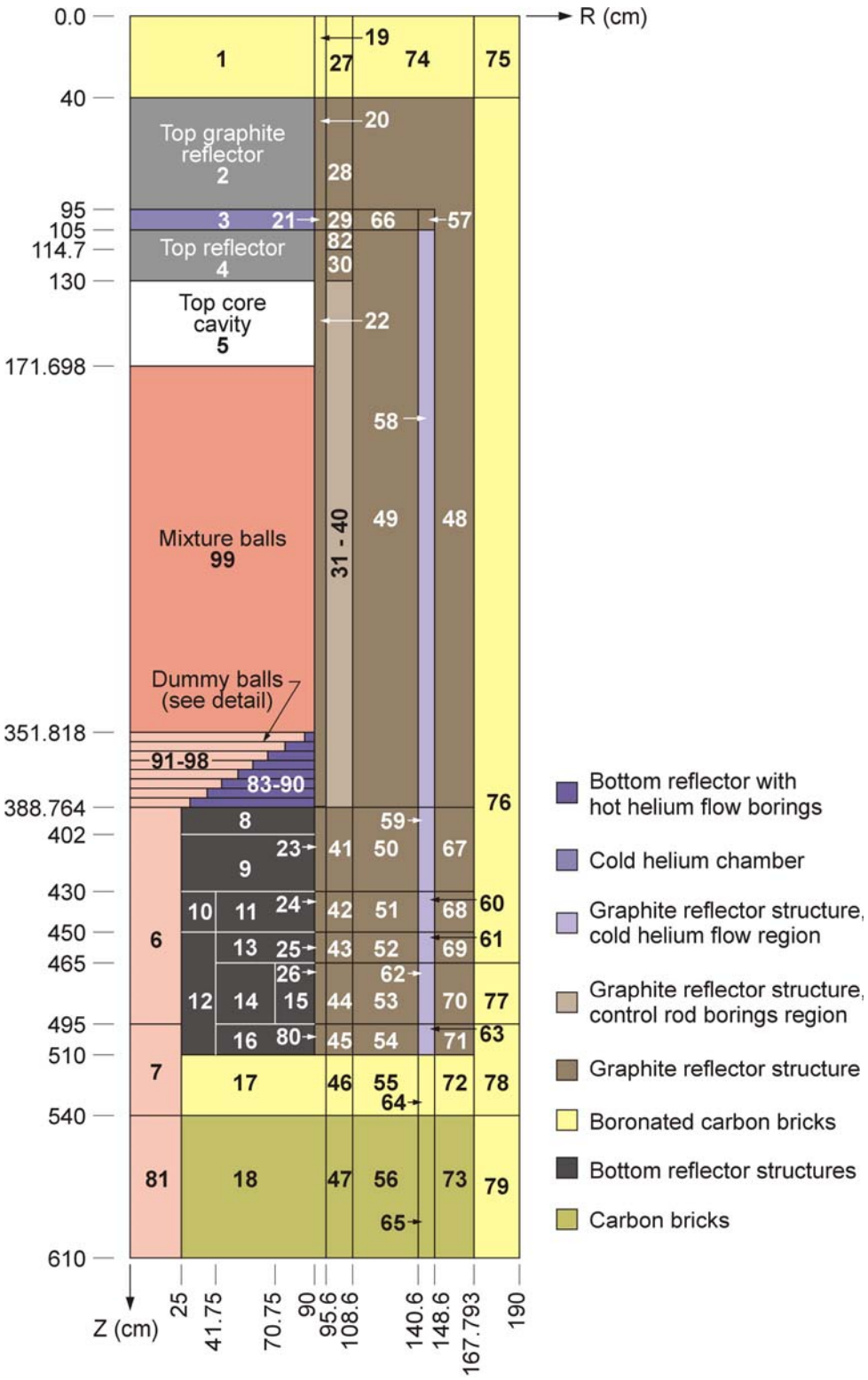

Figure 5(a). Zones of HTR-10 for modeling (dimensions are in cm)

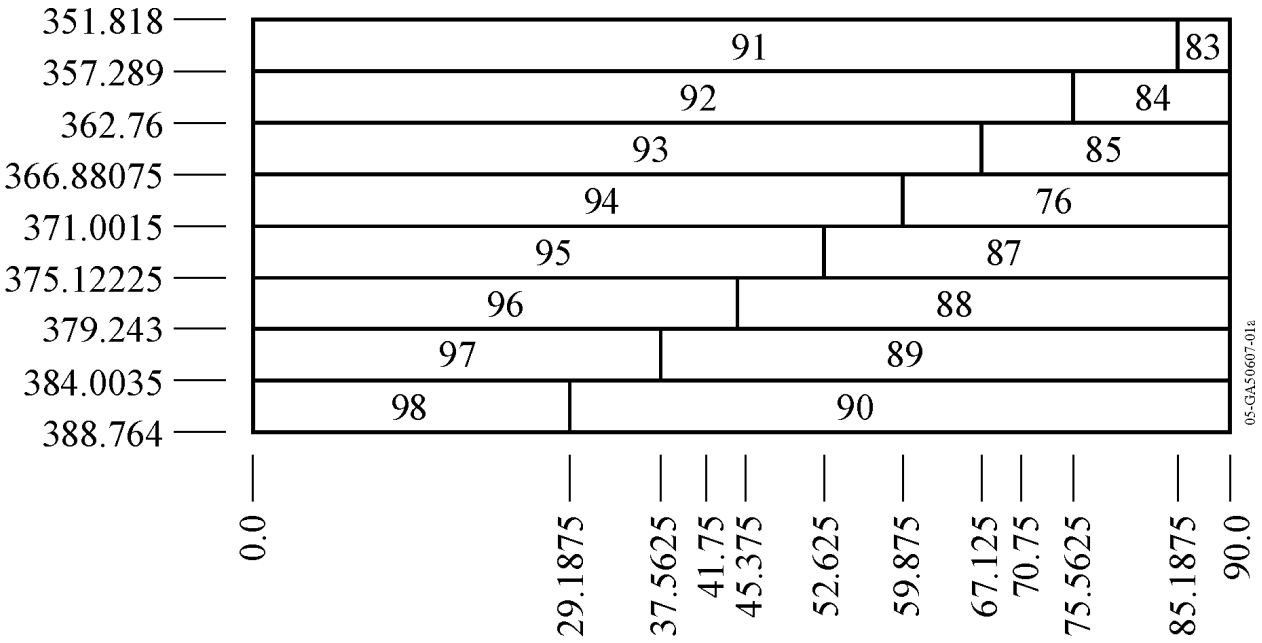

Figure 5(b). Detail in conus region (dimensions are in cm)

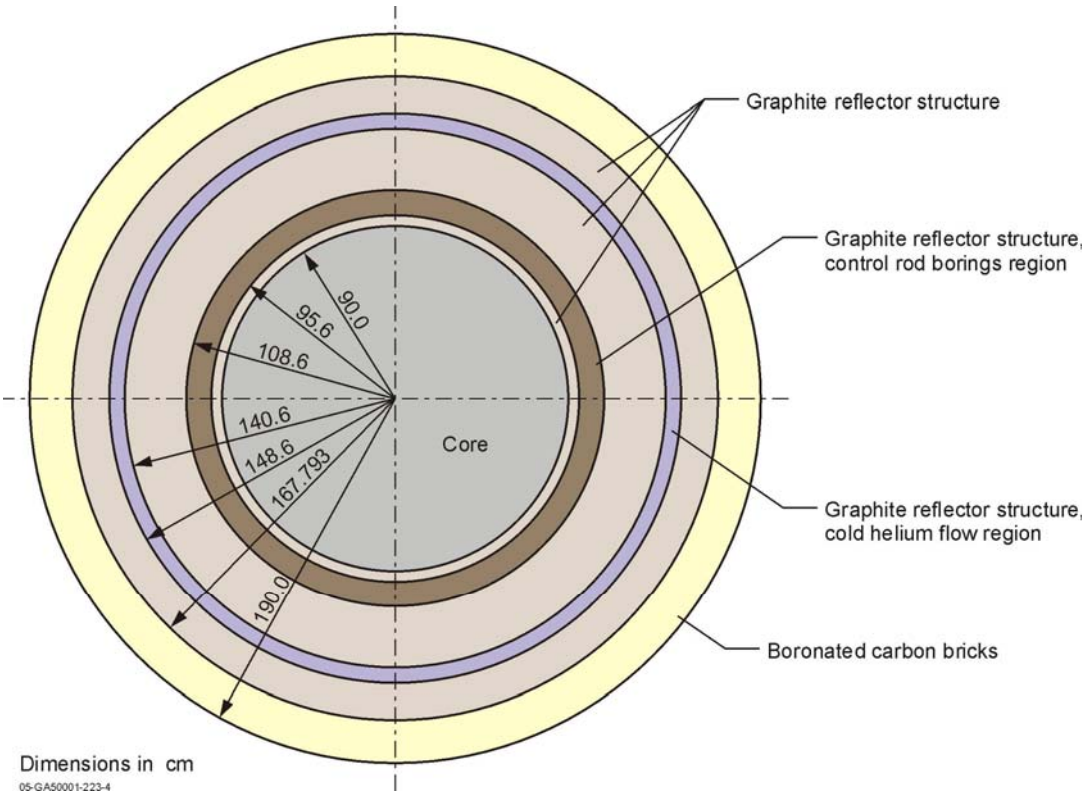

Figure 6. Cross section of reactor in core region

Table 8. Compositions of zones shown in Figure 3 (from Reference 1, with revisions)

No. of zone	Carbon density (a/b-cm)	Natural boron density (a/b-cm)	Remarks
83-90	0.851047E-01	0.456926E-06	Bottom reflector with hot helium flow borings
1	0.729410E-01	0.329811E-02	Boronated carbon bricks
2	0.851462E-01	0.457148E-06	Top graphite reflector
3	0.145350E-01	0.780384E-07	Cold helium chamber
4	0.802916E-01	0.431084E-06	Top reflector
5			Top core cavity
6,7,91-97	0.572501E-01	0.277884E-08	Dummy balls, simplified as graphite of lower density
8	0.781408E-01	0.419537E-06	Bottom reflector structures
9	0.823751E-01	0.442271E-06	Bottom reflector structures
10	0.843647E-01	0.298504E-03	Bottom reflector structures
11	0.817101E-01	0.156416E-03	Bottom reflector structures
12	0.850790E-01	0.209092E-03	Bottom reflector structures
13	0.819167E-01	0.358529E-04	Bottom reflector structures
14	0.541118E-01	0.577456E-04	Bottom reflector structures
15	0.332110E-01	0.178309E-06	Bottom reflector structures
16	0.881811E-01	0.358866E-04	Bottom reflector structures
17,55,72, 74,75,76, 78,79	0.765984E-01	0.346349E-02	Boronated carbon bricks
18,56,73	0.797184E-01	0.000000E+00	Carbon bricks
19	0.761157E-01	0.344166E-02	Boronated carbon bricks
20	0.878374E-01	0.471597E-06	Graphite reflector structure
21	0.579696E-01	0.311238E-06	Graphite reflector structure
22,23,25, 49, 50,52,54, 66, 67,69,71, 80	0.882418E-01	0.473769E-06	Graphite reflector structure
24,51,68	0.879541E-01	0.168369E-03	Graphite reflector structure
26	0.846754E-01	0.454621E-06	Graphite reflector structure
27	0.589319E-01	0.266468E-02	Boronated carbon bricks
28,82	0.678899E-01	1.400000E-05	Graphite reflector structure
29	0.403794E-01	1.400000E-05	Graphite reflector structure
30,41	0.678899E-01	0.364500E-06	Graphite reflector structure
31-40	0.634459E-01	0.340640E-06	Graphite reflector, control rod borings region
42	0.676758E-01	0.125331E-03	Graphite reflector structure
43,45	0.861476E-01	0.462525E-06	Graphite reflector structure
44	0.829066E-01	0.445124E-06	Graphite reflector structure
46	0.747805E-01	0.338129E-02	Boronated carbon bricks
47	0.778265E-01	0.000000E+00	Carbon bricks
48	0.582699E-01	0.312850E-06	Graphite reflector structure
53	0.855860E-01	0.459510E-06	Graphite reflector structure
57	0.728262E-01	0.391003E-06	Graphite reflector structure
58,59,61, 63	0.760368E-01	0.408240E-06	Graphite reflector, cold helium flow region
60	0.757889E-01	0.145082E-03	Graphite reflector, cold helium flow region
62	0.737484E-01	0.395954E-06	Graphite reflector, cold helium flow region
64	0.660039E-01	0.298444E-02	Boronated carbon bricks
65	0.686924E-01	0.000000E+00	Carbon bricks
70	0.861500E-01	0.462538E-06	Graphite reflector structure
77	0.749927E-01	0.339088E-02	Boronated carbon bricks
81	0.847872E-01	0.000000E+00	Dummy balls, but artificially taken as carbon bricks

Table 9. Dimensions of Pebbles and Fuel Particles

Diameter of ball	6.0 cm
Diameter of fuel zone	5.0 cm
Volumetric filling fraction of balls in the core	0.61
Radius of the kernel(mm)	0.25
Coating layer materials (starting from kernel)	Buffer/PyC/SiC/PyC
Coating layer thickness(mm)	0.09/0.04/0.035/0.04
Diameter of dummy (no fuel) elements	6.0 cm

PEBBED is a core design and fuel management tool written to obtain simultaneous solutions of the neutron diffusion equation and the nuclide depletion/production equations in the equilibrium core directly, without following the evolution of the nuclide number densities and the neutron flux in time. PEBBED accounts explicitly for the motion of the fuel and treats arbitrarily specified pebble recirculation patterns. In the HTR-10 startup core, the fuel was not moving; PEBBED also treats this special case.

PEBBED now offers an analytical nodal option for solving the diffusion equation. However, this option had not been fully implemented in *r*-*z* cylindrical geometry when this uncertainty analysis was begun. Therefore, the uncertainty analysis was performed with the older finite-difference option in PEBBED. PEBBED has the capability to perform full *r*-θ-*z* analysis with the finite-difference option, but this uncertainty analysis was done in *r*-*z* geometry. PEBBED will soon have full three-dimensional analytical nodal capability in cylindrical geometry.

Most of the regions in Figure 5 were subdivided into several computational mesh cells in the PEBBED model. The computational mesh can be inferred from the input file in Appendix A. The meshing was selected on the basis of prior experience with spatial convergence in verification and validation studies of PEBBED.

Cross sections for PEBBED were computed by the INL's COMBINE code,[1] so named because it combines the PHROG[2] and INCITE[1] fast and thermal spectrum codes. COMBINE uses a

1 Robert A. Grimesey, David W. Nigg, and Richard L. Curtis, *COMBINE/PC – A Portable ENDF/B Version 5 Neutron Spectrum and Cross-Section Generation Program*, EGG-2589, Rev. 1, Idaho National Engineering Laboratory, February 1991.

(2) R.L. Curtis, et al., *PHROG – A FORTRAN-IV Program to Generate Fast Neutron Spectra and Average Multigroup Constants*, Idaho Nuclear Corp., IN-1435, April 1971.

166-group cross section data base derived from the Evaluated Nuclear Data Files (ENDF/B), Version 6[(2)] over the energy range from 0.001 eV to 16.905 MeV. COMBINE solves the B-1 or B-3 approximations to the neutron transport equation, at the user's choice. The P-1 approximation may be chosen as a special case of the B-1 solution. For this evaluation, the B-1 option was chosen.

COMBINE has been improved numerous times since it was first written. The version used for this evaluation is COMBINE-6.02.[(3)] Footnote (5) is an abbreviated report, mostly containing revised material library labels and revised input instructions. Footnote (1) is still the proper source for detailed theoretical elucidation of COMBINE.

In the HTR-10 startup core, 57% of the pebbles are fuel spheres and 43% are dummy balls. The COMBINE model in the core consists of a fuel sphere surrounded by the corresponding quantities of coolant and dummy-pebble graphite in a homogeneous mixture. The fuel sphere consists of a homogenized fuel zone and a pure graphite zone. A separate COMBINE model was developed for the reflector; the COMBINE calculations in the core and the reflector produce cross sections in the two spectral zones defined in the PEBBED model – i.e., the core spectral zone and the reflector spectral zone. In the reflector, the only materials present are carbon, boron, and coolant. The proportions of carbon and boron are similar except in the boronated carbon bricks used in the outer region where the neutron importance is low. Therefore, the atomic number densities used in the COMBINE reflector model were based on only two of the regions shown in Figure 5, regions 22 and 31. The COMBINE input file for the as-run critical configuration is also contained in Appendix A.

For heterogeneous systems such as PBRs, shadowing effects are accounted for in COMBINE by Dancoff factors. The PBR is doubly heterogeneous, so both interpebble and intrapebble Dancoff factors are required. For this evaluation, the Dancoff factors were computed by the new code PEBDAN, developed at the INL specifically for PBRs by Kloosterman and Ougouag.[(4)] The

---

(1) R. L. Curtis and R. A. Grimesey, *INCITE: A FORTRAN-IV Program to Generate Thermal Neutron Spectra and Multigroup Constants Using Arbitrary Scattering Kernels*, Idaho Nuclear Corporation, IN-1062, 1967.

(2) R. Kinsey, *Data Formats and Procedures for the Evaluated Nuclear Data File ENDF*, Brookhaven National Laboratory, BNL-NCS-50496, 1979.

(3) W. Y. Yoon letter to D. W. Nigg, "COMBINE-6 CYCLE 1," WYY-01-94, January 17, 1994.

(4) J. Kloosterman and A. M. Ougouag, "Computation of Dancoff Factors for Fuel Elements Incorporating Randomly Packed TRISO Particles," INEEL/EXT-05-02593, Idaho National Engineering and Environmental Laboratory, January 2005.

input file for PEBDAN is also included in Appendix A.

COMBINE not only predicts k_∞ for the unit cell, it also predicts k_{eff} for specified values of fast and thermal buckling. Since the actual reactor is critical, the appropriate values of buckling are those for which COMBINE gives k_{eff}=1.0. A search was performed to determine these appropriate values; the result was $B^2=4.958x10^{-4}$ for both the fast and thermal cases.

3.1.2 Dimensions

The dimensions of the model regions are shown in Figure 5. The pebble dimensions are given in Table 9. The dimensions of other regions involved in the uncertainty analysis are given in Table 10. Figure 7 shows the dimensions of the KLAK channels in the core region.

Table 10. Dimensions of regions in HTR-10 not defined elsewhere

Region	Diameter (cm)	Coordinate of center (cm)	Channel length range (cm)
Twenty helium flow channels	8.0	144.6 radius	105.0≤z≤610.0
Ten control rod channels & 3 irradiation channels	13.0	102.1 radius	0≤z≤-450.0
Seven KLAK channels, sections with circular cross section	6.0	98.6 radius	0≤z<-130.0 and 388.764<z≤-610.0
Seven KLAK channels, sections with oval cross section	See Figure 6.	98.6 radius (the long axis of the cross section is in the circumferential direction)	130.0≤z≤-388.764
Hot gas duct	30.0	*z*=480.0	90.0≤*r*≤190.0
Fuel discharge tube	25.0	*r*=0	388.764≤z≤610.0

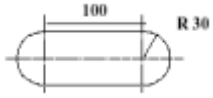

Figure 7. Cross section of KLAK channel in axial zone of the core (dimensions in mm)

3.1.3 Material Data

As shown in Figure 5, the model regions are numbered from 1 to 99. In the model of the initial critical configuration, the control rod regions in Figure 5, labeled 31-40, were consolidated into region 31, leaving a gap from 32-40. (Dividing the control rod region into several model regions allowed partial insertion of control rods, which would be required to evaluate the control rod worth experiment.)

Because the cross sections of the same nuclides will be different in the core and the reflector, which are treated as different spectral zones in the model, nuclides that appear in both zones are treated separately in the two zones, with different material numbers.

The only materials present in the model are graphite (with varying boron concentrations), fuel, and coolant. The reactor vessel and other structural components are omitted. These components are all located in regions of very small neutron importance, so their omission is reasonable. (Perusal of the PEBBED flux output file shows that the thermal neutron flux in the boronated carbon bricks is between four and eleven orders of magnitude lower than that in the core, as depicted in Figure 8; the other neutron energy groups show similar disparities.) The channels for coolant flow, control rods, and KLAK are merely borings in the reflector, so there are no structural materials associated with them.

For the reflector components, the carbon and boron atomic number densities were provided by the HTR-10 group (Reference 1); these densities are presented in Table 8. Only the total boron densities were specified; these were converted to B-10 and B-11 densities by multiplying by the natural abundance (0.199 for B-10 and 0.801 for B-11; cf. the Chart of the Nuclides[1]). The atomic number densities of the gaseous constituents were calculated from the stated temperature and total pressure, 15 °C and 0.1013 MPa, and the assumption that the air is saturated. The proportions of the constituents of dry air are listed below by volume[2]:

Nitrogen 78.084%
Oxygen 20.9476%
Argon 0.934%.

The remaining constituents of dry air are ignored.

The graphite density in regions 22,23,25,48,49,50,52,54,67,69,71,and 80 is solid density (at 1.76 g/cm^3, the specified density of the reflector graphite); the coolant volumes are determined in the other regions as the fractions of the solid density that the graphite in them occupies.

The carbon and boron atomic number densities are also tabulated in Reference 1 for the dummy balls, but the tabulated densities had to be corrected for the as-built composition (1.84 g/cm^3 instead of 1.73 g/cm^3 for carbon and 0.125 ppm instead of 1.3 ppm for boron).

The number densities in the core were calculated from the specifications given in Reference 1. First, a typical cell was defined consisting of 57% of a fuel ball, 43% of a dummy ball, and the

(1) *Chart of the Nuclides*, Thirteenth Edition, General Electric Company, 1984.

(2) http://www.physlink.com/Reference/AirComposition.cfm, citing the CRC Handbook of Chemistry and Physics, David R. Lide, Editor-in-Chief, 1997 Edition.

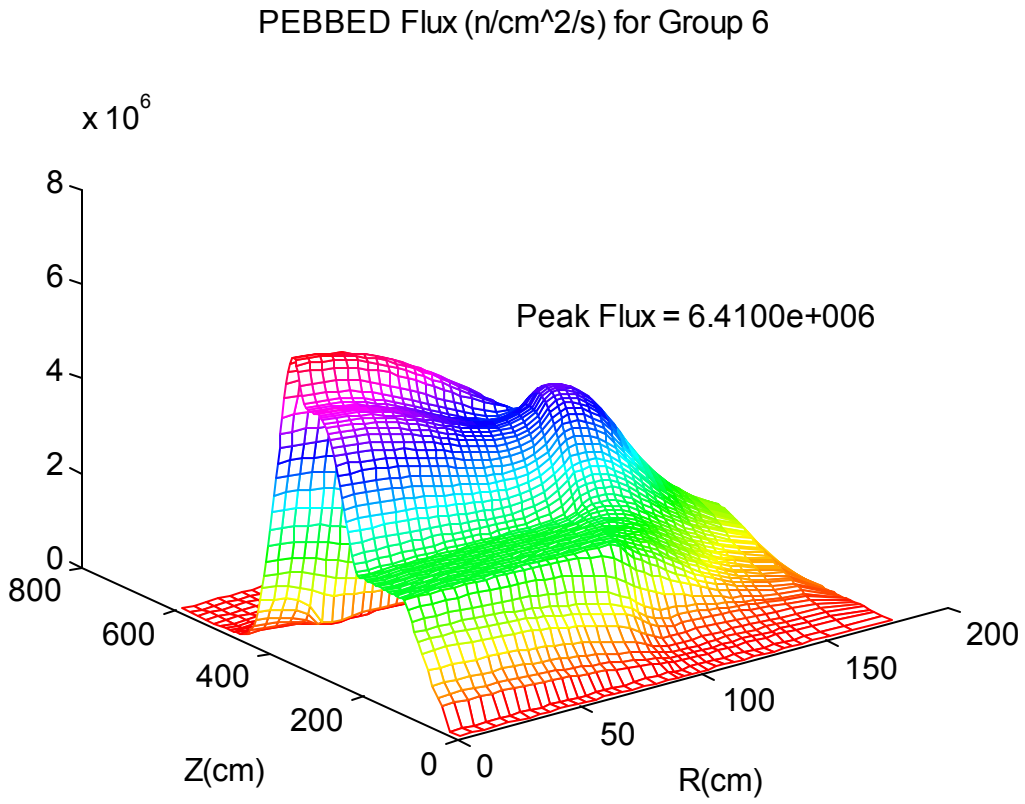

Figure 8. Thermal neutron flux in HTR-10 nominal case (the origin is at the top center of the model)

coolant volume associated with one ball, based on a packing fraction of 61% as stated in Reference 1. The volume of the cell was found to be 185.405 cm^3. Table 11 specifies the dimensions and compositions of all the components in the core region. From these data, one can calculate the average number densities of all the nuclides in the core. Because this calculation is tedious, it is sketched in Appendix B. Table 12 specifies the nominal compositions of the reflector graphite and boronated carbon bricks.

The zone-averaged atomic number densities of all nuclides in all zones in the model are given in the base-case PEBBED input in Appendix A. Tables 13-16 also give the calculated atomic number densities. Table 13 presents the homogenized number densities used in the model. Table 14 gives the number densities in the core components. The values in Table 14 are given for the reader's convenience; they were not used in this uncertainty analysis. Table 15 gives the number densities of the raw materials in the reflector – the solid reflector graphite and boronated carbon materials. Table 16 gives the number densities in air at the experiment conditions.

Table 11. Nominal material properties of fuel and dummy pebbles as built (from Reference 1)

Density of graphite in matrix and outer shell	1.73 g/cm^3
Heavy metal (uranium) loading (weight) per ball	5.0 g
Enrichment of U_{235} (weight)	17 %
Equivalent natural boron content of impurities in uranium	4 ppm
Equivalent natural boron content of impurities in graphite	1.3 ppm
Volumetric filling fraction of balls in the core	0.61
UO2 density(g/cm^3)	10.4
Coating layer materials (starting from kernel)	Buffer/PyC/SiC/PyC
Coating layer density(g/cm^3)	1.1/1.9/3.18/1.9
Density of graphite in dummy balls	1.84 g/cm^3
Equivalent natural boron content of impurities in graphite in dummy balls	0.125 ppm

Table 12. Nominal material properties of reflector materials (from Reference 1)

Density of reflector graphite	1.76 g/cm^3
Equivalent natural boron impurity in reflector graphite	4.8366 ppm
Density of boronated carbon bricks including B_4C	1.59g/cm^3
Weight ratio of B_4C in boronated carbon bricks	5%

Table 13. Homogenized atomic number densities in the model

Nuclide	Atomic number density (a/b-cm)
U-235, averaged over core	6.69520E-6
U-238, averaged over core	3.22755E-5
O-16 in kernels, averaged over core	7.79414E-5
Natural Si, averaged over core	8.51054E-5
Graphite averaged over core	5.40964E-2
B-10 averaged over core	9.92089E-9
B-11 averaged over core	3.99328E-8
Nitrogen averaged over core	1.55875E-5
O-16 in dry air, averaged over core	4.09021E-6
Argon averaged over core	9.11929E-8
Hydrogen averaged over core	3.34631E-7
O-16 from water vapor, averaged over core	1.67316E-7
Graphite at 1.76 g/cm^3	8.82418E-2
B-10 at 4.8366 ppm total boron concentration	9.42800E-8
B-11 at 4.8366 ppm total boron concentration	3.79489E-7

Table 14. Number densities in core components (not homogenized)

Nuclide	Atomic number density (a/b-cm)
U-235 in kernel	3.99198E-3
U-238 in kernel	1.92441E-2
O-16 in kernel	4.64720E-2
B-10 in kernel	4.06384E-7
B-11 in kernel	1.63575E-6
Carbon in buffer	5.51511E-2
B-10 in buffer	1.58513E-8
B-11 in buffer	6.38035E-8
Carbon in IPyC and OPyC	9.52610E-2
B-10 in IPyC and OPyC	2.73795E-8
B-11 in IPyC and OPyC	1.10206E-7
Carbon in SiC	4.77597E-2
Si (nat) in SiC	4.77597E-2
Carbon in fuel matrix	8.67377E-2
B-10 in fuel matrix	2.49298E-8
B-11 in fuel matrix	1.00345E-7
Carbon in dummy balls	9.22528E-2
B-10 in dummy balls	2.54951E-9
B-11 in dummy balls	1.02621E-8

Table 15. Number densities in solid reflector components

Nuclide	Atomic number density (a/b-cm)
Graphite at 1.76 g/cm^3	8.82418E-2
B-10 at 4.8366 ppm total boron concentration	9.42800E-8
B-11 at 4.8366 ppm total boron concentration	3.79489E-7
Carbon in boronated carbon bricks	7.65984E-2
B-10 in boronated carbon bricks	6.89235E-4
B-11 in boronated carbon bricks	2.77426E-2

Table 16. Number densities in air at experiment conditions

Nuclide	Atomic number density (a/b-cm)
Nitrogen in dry air	3.95901E-5
O-16 in dry air	1.06209E-5
Ar in dry air	2.36778E-7
Hydrogen in vapor at saturation	8.58028E-7
O-16 in vapor at saturation	4.29014E-7

3.1.4 Temperature Data

The temperature of the entire system was a uniform 15 °C.

3.1.5 Experimental and Benchmark-Model k_{eff} and / or Subcritical Parameters

The value of k_{eff} is not explicitly given in Reference 1. Instead, the core height at criticality is given. It is implied that k_{eff} is exactly equal to 1 at the measured critical core height of 123.06 cm. The effects of uncertainty in the core height specification, which is equivalent to an uncertainty in the number of pebbles in the core, are discussed in subsection 2.1.1. The approach to criticality was tracked by neutron counters, and a small Am-Be neutron source was used to provide a neutron flux for the counters to track.

3.2 Benchmark-Model Specifications for Buckling and Extrapolation-Length Measurements

No buckling or extrapolation length measurements were made.

3.3 Benchmark-Model Specifications for Spectral Characteristics Measurements

No spectral characteristics were measured.

3.4 Benchmark-Model Specifications for Reactivity Effects Measurements

The control rod worth measurements are not evaluated in this report.

3.5 Benchmark-Model Specifications for Reactivity Coefficient Measurements

No reactivity coefficient measurements were made.

3.6 Benchmark-Model Specifications for Kinetics Measurements

No kinetics parameters were measured.

3.7 Benchmark-Model Specifications for Reaction-Rate Distribution Measurements

No reaction-rate distribution measurements were made.

3.8 Benchmark-Model Specifications for Power Distribution Measurements

No power distribution measurements were made.

3.9 Benchmark-Model Specifications for Isotopic Measurements

No isotopic measurements were made.

3.10 Benchmark-Model Specifications for Other Miscellaneous Types of Measurements

No other measurements have been reported.

4.0 RESULTS OF SAMPLE CALCULATIONS

This section presents the principal results of the calculations described in Section 2. The expected value of k_{eff} is 1.0, but the calculational model gives a value of 1.03257. The uncertainty is given as a percentage deviation from the model result.

4.1 Results of Calculations of the Critical or Subcritical Configurations

As noted above, the baseline value of keff is 1.03257. The deviation from 1.0 is believed to be due to inaccuracies in the cross sections. Whatever the reason, the bias of 0.03257 is carried through the analysis.

Table 7. Principal results of calculations

Case	k_{eff}	100(C-E)/E	Uncertainty (%)
Expected value	1.00000	0.00000	N/A
Base case	1.03257	3.25700	N/A
Overall uncertainty	1.03798*	3.79800	0.52394

*This is the value of k_{eff} at $+1\sigma$. The value at -1σ, 1.02716, is equally valid.

4.2 Results of Buckling and Extrapolation Length Calculations

No buckling or extrapolation length measurements were made.

4.3 Results of Spectral-Characteristics Calculations

No spectral characteristics were measured.

4.4 Results of Reactivity-Effects Calculations

No reactivity effects were calculated.

4.5 Results of Reactivity Coefficient Calculations

No reactivity coefficients were measured.

4.6 Results of Kinetics Parameter Calculations

No kinetics parameters were measured.

4.7 Results of Reaction-Rate Distribution Calculations

No reaction-rate distributions were measured.

4.8 Results of Power Distribution Calculations

No power distributions were measured.

4.9 Results of Isotopic Calculations

Isotopic concentrations were not measured.

4.10 Results of Calculations for Other Miscellaneous Types of Measurements

No other measurements were reported.

5.0 REFERENCES

1. "Evaluation of high temperature gas cooled reactor performance: Benchmark analysis related to initial testing of the HTTR and HTR-10," IAEA-TECDOC-1382, International Atomic Energy Agency, Vienna, November 2003.

2. "Fuel performance and fission product behavior in gas cooled reactors," IAEA-TECDOC-978, International Atomic Energy Agency, Vienna, November, 1927, pp. 11-13.

APPENDICES

APPENDIX A: COMPUTER CODES, CROSS SECTIONS, AND TYPICAL INPUT LISTINGS

The codes used in this evaluation are PEBBED4, COMBINE-6, and PEBDAN. Detailed information on these codes is given in this appendix.

A.1.1 Name(s) of code system(s) used

PEBBED4

COMBINE-6 version 2

COMBDAN

A.1.2 Bibliographic references for the codes used.

H. D. Gougar, W. K. Terry, and A. M. Ougouag, *PEBBED V.4.3 Manual (DRAFT)*, Idaho National Engineering and Environmental Laboratory. This manual has not been published, but it will be provided to officially designated reviewers.
Robert A. Grimesey, David W. Nigg, and Richard L. Curtis, *COMBINE/PC – A Portable ENDF/B Version 5 Neutron Spectrum and Cross-Section Generation Program*, EGG-2589, Rev. 1, Idaho National Engineering Laboratory, February 1991.

W. Y. Yoon letter to D. W. Nigg, "COMBINE-6 CYCLE 1," WYY-01-94, January 17, 1994.

.J. Kloosterman and A. M. Ougouag, "Computation of Dancoff Factors for Fuel Elements Incorporating Randomly Packed TRISO Particles," INEEL/EXT-05-02593, Idaho National Engineering and Environmental Laboratory, January 2005.

R. Kinsey, *Data Formats and Procedures for the Evaluated Nuclear Data File ENDF*, Brookhaven National Laboratory, BNL-NCS-50496, 1979.

A.1.3 Origin of cross-section data

COMBINE uses cross sections from ENDF/B-VI.

A.1.4 Calculational methods used

PEBBED solves the neutron diffusion equation in one-, two-, or three-dimensional cylindrical or Cartesian geometry by finite-difference methods or in one- or two-dimensional cylindrical geometry by nodal methods. In PEBBED, the neutron diffusion equation is solved simultaneously with the nuclide depletion/production equations in a flowing core for a user-specified number of nuclides in the steady-state configuration of neutron flux and composition distribution. It does this by an iterative scheme without following the development of the state of the reactor in time. PEBBED also contains thermohydraulics modules for computing temperatures in normal operation and accident scenarios. However, in this evaluation, only the diffusion-theory component was needed since the fuel was all fresh and the core was stationary. Because the two-dimensional nodal option was not yet working when this evaluation was initiated, the finite-difference option was applied.

COMBINE solves the B-1 or B-3 approximation to the neutron transport equation, or the P-1 approximation as a special case of the B-1 approximation. At the user's option, it can perform an ABH thermal calculation and Nordheim, GAM-1, or Bondarenko treatment of the resolved resonance region. It uses the Wigner Rational Approximation in the unresolved resonance region. In this evaluation, the B-1 approximation was used, and the Nordheim treatment of the unresolved resonance region was chosen. The ABH option was not used. The only fissile nuclide present in the fresh HTR-10 core is u-235, so a U-235 fission spectrum was used. Self-shielding factors were not specified.

COMBINE contains an internal module for computing Dancoff factors to account for shadowing effects in doubly heterogeneous systems like PBRs. However, recent advances in treating such double heterogeneities have led to an improved method of calculating the Dancoff factors. This method is implemented in the PEBDAN code. PEBDAN results were provided as input data to the COMBINE input file.

A.1.5 Energy group structure

COMBINE begins with a 166-group energy structure from ENDF/B-6; in this evaluation, the fine group structure was collapsed to six groups in the following energy ranges:

group 1 16.905-0.111 MeV
group 2 0.111 MeV – 7100 eV
group 3 7100 – 29.0 eV
group 4 29.0 – 2.38 eV
group 5 2.38 – 0.532 eV
group 6 0.532 – 0 eV.

The two groups of lowest energy are the thermal groups.

A.1.6 Component calculations

A.1.6.1 COMBINE core spectrum and cross section calculation

Type of calculation: Unit cell
Geometry: spherical
Theory used: transport
Method used: B-1 approximation, Nordheim numerical method, Wigner rational approximation
Calculation characteristics: spectrum calculation in mixture-ball region of core, cross section calculation for each nuclide in the core (with separate nuclide labels assigned to oxygen in fuel, dry air, and water vapor), resonance materials are U-235 and U-238

A.1.6.2 COMBINE reflector cross section calculation

Type of calculation: coarse-group cross section calculation
Geometry: NA
Theory used: transport
Method used: B_1 approximation
Calculation characteristics: given U-235 fission spectrum, thermal and fast buckling values, compute group microscopic cross sections in reflector materials; no resonance materials are present

A.1.6.3 PEBDAN calculation of Dancoff factors

Type of calculation: computation of Dancoff factors
Geometry: spheres in finite media
Theory used: transport
Method used: Monte Carlo ray tracing
Calculation characteristics: given the fuel particle characteristics and packing fraction, find the intrapebble Dancoff factor; given the pebble characteristics and packing distribution, find the interpebble Dancoff factor

A.1.6.4 PEBBED calculation of k_{eff}

Type of calculation: full reactor
Geometry: cylindrical
Theory used: diffusion
Method used: finite-difference
Calculation characteristics: given detailed description of core and reflector regions, compute k-effective; six energy groups, two thermal groups, homogenized core region, reflector regions defined by HTR-10 group, two spectral zones

A.1.7 Other assumptions and characteristics – see detailed description in Section 3.1

A.1.8 Typical Input Listings for each code system type

A.1.8.1 COMBINE Input Listing

The input listing presented below is the COMBINE input for the configuration experimentally measured to be critical. It includes sections for both the core and reflector regions.

```
=  HTR-10 Spectral Zone Computation with 25mm (o.r.) fuel region   17% enrichment by wt WKT 9 Sept 05
=  Two Spectral Zones
=  Spectrum calculation and core zone
=  COMBINE V5.23 Conversion (DWN) back to v6.02 (wkt)
=  As run with moist air coolant, 15 deg C, p tot = 0.1013 MPa
1010101   0 0 1  1 12 6 1 -1 1 0 0 0 0 54 3 100
1010102   0 0 0 0
1010201   166 144 133 111 101 54
1020101   1 1 0 0 0 0 0 0 0 0 0 0
1030101   4 0 0 0 0 0 0
1030201   2 1         *U-235
1030202   2 2         *U-238
1030203   2 3         *O-16 in UO2 at 296 K
1030204   2 4         *Silicon
1030205   2 5         *Graphite in core at 296 K
1030206   2 6         *Core Boron-10
1030207   2 7         *Core Boron-11
1030208   2 8         *Core Nitrogen
1030209   2 9         *Oxygen in dry air in core
1030210   2 10        *Argon in core
1030211   2 11        *H in H2O vapor in core at 296 K
1030212   2 12        *Oxygen in water vapor in core
1041001   4.958E-4 4.958E-4  288.15         *SPECT AT 15 deg C
1042001   9228.0 92.23501  6.69520E-06 0.0 3.3333E-02 0.2318 *U-235
1042002   9237.0 92.23801  3.22755E-05 0.0 3.3333E-02 0.2318 *U-238
1042003   825.0  8.01601   7.79414E-05 0.0 3.3333E-02 0.2318 *O-16 in UO2 at 296 K
1042004   1400.0 14.00001  8.51054E-05 0.0 3.3333E-02 0.2318 *Silicon
1042005   600.0  6.01201   5.40718E-02 0.0 3.3333E-02 0.2318 *Graphite in core at 296 K
1042006   525.0  5.01001   9.92089E-09 0.0 3.3333E-02 0.2318 *Boron-10 in core
1042007   528.0  5.01101   3.99328E-08 0.0 3.3333E-02 0.2318 *Boron-11 in core
1042008   725.0  7.01401   1.51624E-05 0.0 3.3333E-02 0.2318 *Nitrogen in core
1042009   825.0  8.01601   4.06762E-06 0.0 3.3333E-02 0.2318 *O-16 in dry air in core at 296 K
1042010   1837.0 18.04001  9.06821E-08 0.0 3.3333E-02 0.2318 *Argon in core
1042011   125.0  1.01801   3.34631E-07 0.0 3.3333E-02 0.2318 *H in H2O vapor in core at 296 K
1042012   825.0  8.01601   1.67316E-07 0.0 3.3333E-02 0.2318 *O-16 in H2O vapor in core at 296 K
1043011   293.0  3.0 3.29243E-05 2.50  0.2634 -1.0  8.54441E-02  *U-235
1043012   4.22952E-04 3.87344E-04  600.0 1400.0  825.0 0.0 0.0
1043021   293.0  3.0 1.60748E-04 2.50  0.2634 -1.0  8.54441E-02  *U-238
```

```
1043022   4.22952E-04 3.87344E-04  600.0 1400.0  825.0 0.0 0.0
.
=HTR-10 6-Group Cross Sections 17% enriched, thermal<0.876eV, fast>0.10eV
=Reflector Spectral Zone
=Updated with moist air coolant
=1010101   0 0 1 1 8 6 1 1 1 0 0 0 0 54 1 100
1010101   0 0 1 1 9 6 1 -1 1 0 0 0 0 54 1 100
1010201   166 144 133 111 101 54
1030101   4 0 0 0 0 0 0
1030201   2 13     *Reflector Graphite at 296 K
1030202   2 14     *Reflector Boron-10
1030203   2 15     *Reflector Boron-11
1030204   2 16     *Nitrogen in reflector
1030205   2 17     *O-16 in dry air in reflector at 296 K
1030206   2 18     *Argon in reflector
1030207   2 19     *H in H2O vapor in reflector at 296 K
1030208   2 20     *O-16 in H2O vapor in reflector at 296 k
1030209   0 21     *U-235 for spectrum
1041001   4.965E-4 4.965E-4  288.15          *SPECT AT 15 deg C
1042001   600.0  6.01201   7.04227E-02 0.0 *Reflector Graphite at 296 K
1042002   525.0  5.01001   7.52415E-08 0.0 *Reflector Boron-10
1042003   528.0  5.01101   3.02857E-07 0.0 *Reflector Boron-11
1042004   725.0  7.01401   7.86E-06    0.0 *Nitrogen in reflector
1042005   825.0  8.01601   2.10E-06    0.0 *O-16 in dry air in reflector at 296 K
1042006   1837.0 18.04001  4.70E-08    0.0 *Argon in reflector
1042007   125.0  1.01801   1.73E-07    0.0 *H in H2O vapor in reflector at 296 K
1042008   825.0  8.01601   8.64E-08    0.0 *O-16 in H2O vapor in reflector at 296 K
1042009   9228.0 92.23501  1.0E-15     0.0 *U-235 to generate spectrum
.
```

A.1.8.2 PEBDAN Input Listing

The input listing presented below is the PEBDAN input.

```
MODULE Constants
  IMPLICIT NONE
  !==============================
  ! Input on fuel and core design
  !==============================
  ! HTR-10
  INTEGER, PARAMETER::npart   = 8335      ! number of particles per standard pebble
  REAL, PARAMETER::radgrn1    = 0.025     ! fuel kernel radis (cm)
  REAL, PARAMETER::radpeb1    = 2.5       ! inner zone radius (cm)
  REAL, PARAMETER::radpeb2    = 3.0       ! outer pebble radius (cm)
  REAL, PARAMETER::radref     = 0.0     ! radius of cylindrical inner reflector (cm)
  REAL, PARAMETER::radcore    = 90.0                ! radius of the core (cm)
  REAL, PARAMETER::hgtcore    = 180.118             ! height of the core (cm)
  !=======================================
  ! Input for generation pebble coordinates
  !=======================================
  REAL, PARAMETER::randpf     = 0.61      ! theoretical packing fraction of a randomly packed bed
  INTEGER, PARAMETER::nranpeb = 200000              ! number of random points per pebble generated
```

```
!=========================================
! Input for calculation of Dancoff Factors
!=========================================
REAL, PARAMETER::sigmod     = 0.4097     ! macroscopic cross section moderator (1/cm)
REAL, PARAMETER::fuelfrac   = 0.57       ! fraction of fuel pebbles, remainder are graphite pebbles
REAL, PARAMETER::threshold  = 0.001      ! threshold for russian roulette in Dancoff calculation
INTEGER, PARAMETER::nrad    = 10         ! number of equi-volume core shells in Dancoff calculation
INTEGER, PARAMETER::nhgt    = 10         ! number of equi-volume core layers in Dancoff calculation
INTEGER, PARAMETER::nbat    = 10         ! number of batches during ray tracing in Dancoff calculation
INTEGER, PARAMETER::nray    = 100        ! number of rays per batch during ray tracing
INTEGER, PARAMETER::nipf    = 200        ! number of intervals in the packing fraction calculation

!=======================================
! Some remaining general input parameters
!=======================================
INTEGER, PARAMETER::lunout  = 6          ! unit for formatted output
INTEGER, PARAMETER::lunpeb  = 10         ! unit for input/output of pebble coordinates
INTEGER, PARAMETER::lunpak  = 11         ! unit for output packing fraction
INTEGER, PARAMETER::lundan  = 12         ! unit for output Dancoff factors
INTEGER, PARAMETER::lunplt  = 13         ! unit for plot output

!===========================================
! Parameters derived from the input parameters
!===========================================
REAL, PARAMETER::diampeb1   = 2*radpeb1
REAL, PARAMETER::diampeb2   = 2*radpeb2
REAL, PARAMETER::diampeb12  = diampeb1**2
REAL, PARAMETER::diampeb22  = diampeb2**2
REAL, PARAMETER::diamcore   = 2*radcore
REAL, PARAMETER::radgrn12   = radgrn1**2
REAL, PARAMETER::radpeb12   = radpeb1**2
REAL, PARAMETER::radpeb13   = radpeb1**3
REAL, PARAMETER::radpeb22   = radpeb2**2
REAL, PARAMETER::radpeb23   = radpeb2**3
REAL, PARAMETER::radcore2   = radcore**2
REAL, PARAMETER::radref2    = radref**2
REAL, PARAMETER::radinn     = radref+radpeb2
REAL, PARAMETER::radinn2    = radinn**2
REAL, PARAMETER::radout     = radcore-radpeb2
REAL, PARAMETER::radout2    = radout**2
REAL, PARAMETER::sigfuel    = 0.75*npart*radgrn12/radpeb13
REAL, PARAMETER::pi         = 3.14159265359
REAL, PARAMETER::halfpi     = 0.5*pi
REAL, PARAMETER::twopi      = 2*pi
REAL, PARAMETER::fourpi     = 4*pi
REAL, PARAMETER::big        = 1.0E30
REAL, PARAMETER::eps        = 1.0E-30
REAL, PARAMETER::twoeps     = 2*eps
REAL, PARAMETER::small      = 2.0E-2                ! criterion for squared overlap of pebbles
! npeb is the number of pebbles that fit theoretically in the core volume
! npeb can be less than the number of pebbles in the file,
!      then more pebble coordinates need to be generated (a kind of restart)
! npeb can be larger then the number of pebbles in the file,
```

```
 !      then only a part of the file need to be read
 ! The actual number of pebbles read always becomes "np"
  INTEGER, PARAMETER::npeb    = INT(randpf*(radcore2-radref2)*hgtcore/radpeb23)
END MODULE Constants
```

A.1.8.3 PEBBED Input Listing

The following listing is the PEBBED input for the configuration that was measured as critical by the HTR-10 group.

```
00001  HTR-10 R-Z 6-Group Critical As Run - Final corrected compositions, 17 wt %
=     ptyp ndim geo sdim NR NQ NZ
00002  1  2  1  2  40  1  99
=       R   Q   Z
00003  1 0 1 1 0 0
00004  5 2 100 1000 20 12 10
00005  1.E-4 1.0-8 1.0E-4 1.0E-4 0.2 0.1 1.0E-4
00006  1 0 0
=      ngr  ntg  infuel  inpres
00007  6     2     2      0
00008  0.95051 0.047997 1.4854E-03 5.0481E-06 0.0 0.0
00009  1.6905E7 1.1109E5 7102. 29.0232 2.38237 0.532
=
00010  21 99 3 0
00011  1.6 1.0
00015  4 0 0 0 0 0
=
00040  0
00060  0.000001  0.0
=      No pebble flow
00070  0.0  0.0
=
=            Radial mesh
00101  5 5 5.0 4 4.1875 8 3.625 4 4.8125 2 2.8
00102  5 4 3.25 8 4.0 2 4.0 2 9.5965 1 22.207
=
=      Azimuthal mesh
00201  1 1 360.
=
=      Axial mesh
00301  4 2 20.0 5 11.0 1 10.0 2 4.85
00302  4 2 7.65 18 5.48656 30 4.102 4 2.7355
00303  4 4 4.12075 2 4.7605 4 3.309 7 4.0
00304  4 4 5.0 2 7.5 4 7.5 2 7.5
00305  2 2 15.0 4 17.5
=
00500  1  1  21  61
00501  22
=
= Pebble Specifications
00700  2 1
00701  100.0 100.0
00702  FUEL  DUMMY
```

```
00703  90.8  0.0
00704  1 2
00705  0 0
=
= alphapo: each row must add to 1
00708  1.0 0.0
=
00710  0.0 0.0
00712  8335.0  0.0
=
= Composition Map
=            R     Q    Z
01201  1  1   1 21  1 1  1  2
01202  1  2   1 21  1 1  3  7
01203  1  3   1 21  1 1  8  8
01204  1  4   1 21  1 1  9 12
01205  1  5   1 21  1 1 13 30
01206  1  6   1  5  1 1 71 91
01207  1  7   1  5  1 1 92 95
01208  1  8   6 21  1 1 71 74
01209  1  9   6 21  1 1 75 81
01210  1 10   6  9  1 1 82 85
01211  1 11  10 21  1 1 82 85
01212  1 12   6  9  1 1 86 93
01213  1 13  10 21  1 1 86 87
01214  1 14  10 17  1 1 88 91
01215  1 15  18 21  1 1 88 91
01216  1 16  10 21  1 1 92 93
01217  1 17   6 23  1 1 94 95
01218  1 18   6 23  1 1 96 99
01219  1 19  22 23  1 1  1  2
01220  1 20  22 23  1 1  3  7
01221  1 21  22 23  1 1  8  8
01222  1 22  22 23  1 1  9 70
01223  1 23  22 23  1 1 71 81
01224  1 24  22 23  1 1 82 85
01225  1 25  22 23  1 1 86 87
01226  1 26  22 23  1 1 88 91
01227  1 27  24 27  1 1  1  2
01228  1 28  24 27  1 1  3  7
01229  1 29  24 27  1 1  8  8
01230  1 30  24 27  1 1 11 12
01231  1 31  24 27  1 1 13 70
01241  1 41  24 27  1 1 71 81
01242  1 42  24 27  1 1 82 85
01243  1 43  24 27  1 1 86 87
01244  1 44  24 27  1 1 88 91
01245  1 45  24 27  1 1 92 93
01246  1 46  24 27  1 1 94 95
01247  1 47  24 27  1 1 96 99
01248  1 48  28 39  1 1  3 70
01249  1 49  28 35  1 1  9 70
01250  1 50  28 35  1 1 71 81
```

```
01251  1 51  28 35  1 1 82 85
01252  1 52  28 35  1 1 86 87
01253  1 53  28 35  1 1 88 91
01254  1 54  28 35  1 1 92 93
01255  1 55  28 35  1 1 94 95
01256  1 56  28 35  1 1 96 99
01257  1 57  36 37  1 1  8  8
01258  1 58  36 37  1 1  9 70
01259  1 59  36 37  1 1 71 81
01260  1 60  36 37  1 1 82 85
01261  1 61  36 37  1 1 86 87
01262  1 62  36 37  1 1 88 91
01263  1 63  36 37  1 1 92 93
01264  1 64  36 37  1 1 94 95
01265  1 65  36 37  1 1 96 99
01266  1 66  28 35  1 1  8  8
01267  1 67  38 39  1 1 71 81
01268  1 68  38 39  1 1 82 85
01269  1 69  38 39  1 1 86 87
01270  1 70  38 39  1 1 88 91
01271  1 71  38 39  1 1 92 93
01272  1 72  38 39  1 1 94 95
01273  1 73  38 39  1 1 96 99
01274  1 74  28 39  1 1  1  2
01275  1 75  40 40  1 1  1  2
01276  1 76  40 40  1 1  3 87
01277  1 77  40 40  1 1 88 91
01278  1 78  40 40  1 1 92 95
01279  1 79  40 40  1 1 96 99
01280  1 80  22 23  1 1 92 93
01281  1 81   1  5  1 1 96 99
01282  1 82  24 27  1 1  9 10
01283  1 83  21 21  1 1 61 62
01284  1 84  19 21  1 1 63 64
01285  1 85  17 21  1 1 65 65
01286  1 86  15 21  1 1 66 66
01287  1 87  13 21  1 1 67 67
01288  1 88  11 21  1 1 68 68
01289  1 89   9 21  1 1 69 69
01290  1 90   7 21  1 1 70 70
01291  1 91   1 20  1 1 61 62
01292  1 92   1 18  1 1 63 64
01293  1 93   1 16  1 1 65 65
01294  1 94   1 14  1 1 66 66
01295  1 95   1 12  1 1 67 67
01296  1 96   1 10  1 1 68 68
01297  1 97   1  8  1 1 69 69
01298  1 98   1  6  1 1 70 70
01299  1 99   1 21  1 1 31 60
=
= Spectral Zone Assignment
01401  1  2   1 40  1 1  1 99
01402  1  3   1 21  1 1 21 60
```

```
=
= Zone Temperatures (deg. C)
01500  20.0
01501  2  2  20.0  3  20.0
=
= Combine Cross-Sections for HTR-10 6-Group
=
=    Generated on 09/09/2005
=
21100   H in H
21110     1.01 0.0000E+00 0.0000E+00 0.0000E+00 0.0000E+00
21101  2.6165E+00 4.2799E-05 0.0000E+00 0.0000E+00
21102  5.6099E+00 2.7738E-04 0.0000E+00 0.0000E+00
21103  6.7492E+00 3.2373E-03 0.0000E+00 0.0000E+00
21104  6.8306E+00 1.9218E-02 0.0000E+00 0.0000E+00
21105  9.3640E+00 5.1221E-02 0.0000E+00 0.0000E+00
21106  2.9322E+01 2.1686E-01 0.0000E+00 0.0000E+00
21111  3.6327E+00 2.0689E+00 1.4079E-01 5.3227E-04 3.5440E-05 9.0480E-06
21121  0.0000E+00 1.0715E+01 6.0162E+00 2.2662E-02 1.5747E-03 4.4902E-04
21131  0.0000E+00 0.0000E+00 1.6754E+01 3.2268E+00 2.2411E-01 6.4455E-02
21141  0.0000E+00 0.0000E+00 0.0000E+00 1.3179E+01 5.6608E+00 1.6281E+00
21151  0.0000E+00 0.0000E+00 0.0000E+00 0.0000E+00 1.1938E+01 9.4635E+00
21161  0.0000E+00 0.0000E+00 0.0000E+00 0.0000E+00 1.2365E-02 3.9377E+01
=
20600   B-10 i
20610    10.01 0.0000E+00 0.0000E+00 0.0000E+00 0.0000E+00
20601  3.1081E+00 7.3837E-01 0.0000E+00 0.0000E+00
20602  5.9186E+00 3.7928E+00 0.0000E+00 0.0000E+00
20603  3.9147E+01 3.7166E+01 0.0000E+00 0.0000E+00
20604  2.2395E+02 2.2196E+02 0.0000E+00 0.0000E+00
20605  5.9336E+02 5.9136E+02 0.0000E+00 0.0000E+00
20606  2.5054E+03 2.5034E+03 0.0000E+00 0.0000E+00
20611  2.5682E+00 1.3320E-01 5.9149E-07 4.2445E-10 0.0000E+00 0.0000E+00
20621  0.0000E+00 2.1323E+00 1.3877E-01 0.0000E+00 0.0000E+00 0.0000E+00
20631  0.0000E+00 0.0000E+00 2.0567E+00 6.7179E-02 0.0000E+00 0.0000E+00
20641  0.0000E+00 0.0000E+00 0.0000E+00 1.9877E+00 1.5216E-01 0.0000E+00
20651  0.0000E+00 0.0000E+00 0.0000E+00 0.0000E+00 2.1420E+00 0.0000E+00
20661  0.0000E+00 0.0000E+00 0.0000E+00 0.0000E+00 0.0000E+00 2.1435E+00
=
20700   B-11 i
20710    11.01 0.0000E+00 0.0000E+00 0.0000E+00 0.0000E+00
20701  2.6964E+00 2.2159E-05 0.0000E+00 0.0000E+00
20702  4.5932E+00 1.0174E-04 0.0000E+00 0.0000E+00
20703  4.5444E+00 5.2749E-05 0.0000E+00 0.0000E+00
20704  4.5447E+00 3.1871E-04 0.0000E+00 0.0000E+00
20705  4.5452E+00 8.4838E-04 0.0000E+00 0.0000E+00
20706  4.5480E+00 3.5894E-03 0.0000E+00 0.0000E+00
20711  2.8370E+00 1.8161E-01 6.0275E-07 9.5296E-11 0.0000E+00 0.0000E+00
20721  0.0000E+00 4.5839E+00 2.9026E-01 0.0000E+00 0.0000E+00 0.0000E+00
20731  0.0000E+00 0.0000E+00 4.7010E+00 1.3901E-01 0.0000E+00 0.0000E+00
20741  0.0000E+00 0.0000E+00 0.0000E+00 4.5254E+00 3.1456E-01 0.0000E+00
20751  0.0000E+00 0.0000E+00 0.0000E+00 0.0000E+00 4.8400E+00 0.0000E+00
20761  0.0000E+00 0.0000E+00 0.0000E+00 0.0000E+00 0.0000E+00 4.8400E+00
```

```
=
20500   Graphi
20510    12.00 0.0000E+00 0.0000E+00 0.0000E+00 0.0000E+00
20501  2.7220E+00 2.9868E-04 0.0000E+00 0.0000E+00
20502  4.3239E+00 1.9843E-06 0.0000E+00 0.0000E+00
20503  4.4674E+00 3.4623E-05 0.0000E+00 0.0000E+00
20504  4.4738E+00 1.9630E-04 0.0000E+00 0.0000E+00
20505  4.4861E+00 5.2440E-04 0.0000E+00 0.0000E+00
20506  4.8054E+00 2.2057E-03 0.0000E+00 0.0000E+00
20511  2.8240E+00 1.6487E-01 4.1034E-07 4.3954E-10 0.0000E+00 0.0000E+00
20521  0.0000E+00 4.3450E+00 2.5981E-01 0.0000E+00 0.0000E+00 0.0000E+00
20531  0.0000E+00 0.0000E+00 4.6081E+00 1.2538E-01 0.0000E+00 0.0000E+00
20541  0.0000E+00 0.0000E+00 0.0000E+00 4.4552E+00 2.8390E-01 0.0000E+00
20551  0.0000E+00 0.0000E+00 0.0000E+00 0.0000E+00 4.2776E+00 4.6085E-01
20561  0.0000E+00 0.0000E+00 0.0000E+00 0.0000E+00 5.1482E-03 4.8199E+00
=
20800   Nitrog
20810    14.00 0.0000E+00 0.0000E+00 0.0000E+00 0.0000E+00
20801  2.2369E+00 6.2977E-02 0.0000E+00 0.0000E+00
20802  6.0554E+00 1.9237E-03 0.0000E+00 0.0000E+00
20803  9.1713E+00 1.8428E-02 0.0000E+00 0.0000E+00
20804  9.5425E+00 1.1009E-01 0.0000E+00 0.0000E+00
20805  9.7369E+00 2.9322E-01 0.0000E+00 0.0000E+00
20806  1.0863E+01 1.2406E+00 0.0000E+00 0.0000E+00
20811  2.2659E+00 1.3331E-01 6.4639E-08 1.4682E-11 0.0000E+00 0.0000E+00
20821  0.0000E+00 6.0358E+00 4.0103E-01 0.0000E+00 0.0000E+00 0.0000E+00
20831  0.0000E+00 0.0000E+00 9.3932E+00 2.2605E-01 0.0000E+00 0.0000E+00
20841  0.0000E+00 0.0000E+00 0.0000E+00 9.3955E+00 5.1269E-01 0.0000E+00
20851  0.0000E+00 0.0000E+00 0.0000E+00 0.0000E+00 9.9201E+00 0.0000E+00
20861  0.0000E+00 0.0000E+00 0.0000E+00 0.0000E+00 0.0000E+00 1.0109E+01
=
20300   O-16 i
20310    15.99 0.0000E+00 0.0000E+00 0.0000E+00 0.0000E+00
20301  3.1852E+00 3.8153E-03 0.0000E+00 0.0000E+00
20302  3.6967E+00 1.9010E-06 0.0000E+00 0.0000E+00
20303  3.7237E+00 3.2161E-06 0.0000E+00 0.0000E+00
20304  3.7248E+00 1.1422E-05 0.0000E+00 0.0000E+00
20305  2.1938E+00 2.9528E-05 0.0000E+00 0.0000E+00
20306  3.7890E+00 1.2418E-04 0.0000E+00 0.0000E+00
20311  3.4212E+00 1.1220E-01 9.6106E-08 1.3497E-11 0.0000E+00 0.0000E+00
20321  0.0000E+00 3.6391E+00 1.6315E-01 0.0000E+00 0.0000E+00 0.0000E+00
20331  0.0000E+00 0.0000E+00 3.8070E+00 7.8163E-02 0.0000E+00 0.0000E+00
20341  0.0000E+00 0.0000E+00 0.0000E+00 3.7111E+00 1.7717E-01 0.0000E+00
20351  0.0000E+00 0.0000E+00 0.0000E+00 0.0000E+00 1.8844E+00 3.3018E-01
20361  0.0000E+00 0.0000E+00 0.0000E+00 0.0000E+00 4.6017E-03 3.9510E+00
=
20900   O-16 i
20910    15.99 0.0000E+00 0.0000E+00 0.0000E+00 0.0000E+00
20901  3.1881E+00 3.8153E-03 0.0000E+00 0.0000E+00
20902  3.6967E+00 1.9010E-06 0.0000E+00 0.0000E+00
20903  3.7237E+00 3.2161E-06 0.0000E+00 0.0000E+00
20904  3.7248E+00 1.1422E-05 0.0000E+00 0.0000E+00
20905  2.1938E+00 2.9528E-05 0.0000E+00 0.0000E+00
```

```
20906  3.7890E+00 1.2418E-04 0.0000E+00 0.0000E+00
20911  3.4256E+00 1.1220E-01 9.6106E-08 1.3497E-11 0.0000E+00 0.0000E+00
20921  0.0000E+00 3.6391E+00 1.6315E-01 0.0000E+00 0.0000E+00 0.0000E+00
20931  0.0000E+00 0.0000E+00 3.8070E+00 7.8163E-02 0.0000E+00 0.0000E+00
20941  0.0000E+00 0.0000E+00 0.0000E+00 3.7111E+00 1.7717E-01 0.0000E+00
20951  0.0000E+00 0.0000E+00 0.0000E+00 0.0000E+00 1.8844E+00 3.3018E-01
20961  0.0000E+00 0.0000E+00 0.0000E+00 0.0000E+00 4.6017E-03 3.9510E+00
=
21200   O-16 i
21210    15.99 0.0000E+00 0.0000E+00 0.0000E+00 0.0000E+00
21201  3.1881E+00 3.8153E-03 0.0000E+00 0.0000E+00
21202  3.6967E+00 1.9010E-06 0.0000E+00 0.0000E+00
21203  3.7237E+00 3.2161E-06 0.0000E+00 0.0000E+00
21204  3.7248E+00 1.1422E-05 0.0000E+00 0.0000E+00
21205  2.1938E+00 2.9528E-05 0.0000E+00 0.0000E+00
21206  3.7890E+00 1.2418E-04 0.0000E+00 0.0000E+00
21211  3.4256E+00 1.1220E-01 9.6106E-08 1.3497E-11 0.0000E+00 0.0000E+00
21221  0.0000E+00 3.6391E+00 1.6315E-01 0.0000E+00 0.0000E+00 0.0000E+00
21231  0.0000E+00 0.0000E+00 3.8070E+00 7.8163E-02 0.0000E+00 0.0000E+00
21241  0.0000E+00 0.0000E+00 0.0000E+00 3.7111E+00 1.7717E-01 0.0000E+00
21251  0.0000E+00 0.0000E+00 0.0000E+00 0.0000E+00 1.8844E+00 3.3018E-01
21261  0.0000E+00 0.0000E+00 0.0000E+00 0.0000E+00 4.6017E-03 3.9510E+00
=
20400   Si-28
20410    27.98 0.0000E+00 0.0000E+00 0.0000E+00 0.0000E+00
20401  2.8985E+00 4.6662E-03 0.0000E+00 0.0000E+00
20402  1.9813E+00 3.0649E-03 0.0000E+00 0.0000E+00
20403  2.0349E+00 2.1954E-03 0.0000E+00 0.0000E+00
20404  2.0176E+00 9.3001E-03 0.0000E+00 0.0000E+00
20405  2.0179E+00 2.4785E-02 0.0000E+00 0.0000E+00
20406  2.0978E+00 1.0468E-01 0.0000E+00 0.0000E+00
20411  3.6411E+00 1.6969E-02 2.4295E-04 8.7372E-08 0.0000E+00 0.0000E+00
20421  0.0000E+00 2.0192E+00 4.9657E-02 0.0000E+00 0.0000E+00 0.0000E+00
20431  0.0000E+00 0.0000E+00 2.0605E+00 2.4211E-02 0.0000E+00 0.0000E+00
20441  0.0000E+00 0.0000E+00 0.0000E+00 2.0037E+00 5.3928E-02 0.0000E+00
20451  0.0000E+00 0.0000E+00 0.0000E+00 0.0000E+00 2.0420E+00 0.0000E+00
20461  0.0000E+00 0.0000E+00 0.0000E+00 0.0000E+00 0.0000E+00 2.0420E+00
=
21000   Argon
21010    39.95 0.0000E+00 0.0000E+00 0.0000E+00 0.0000E+00
21001  0.0000E+00 0.0000E+00 0.0000E+00 0.0000E+00
21002  0.0000E+00 0.0000E+00 0.0000E+00 0.0000E+00
21003  0.0000E+00 0.0000E+00 0.0000E+00 0.0000E+00
21004  0.0000E+00 0.0000E+00 0.0000E+00 0.0000E+00
21005  1.0181E-01 1.0181E-01 0.0000E+00 0.0000E+00
21006  4.3086E-01 4.3086E-01 0.0000E+00 0.0000E+00
21011  0.0000E+00 0.0000E+00 0.0000E+00 0.0000E+00 0.0000E+00 0.0000E+00
21021  0.0000E+00 0.0000E+00 0.0000E+00 0.0000E+00 0.0000E+00 0.0000E+00
21031  0.0000E+00 0.0000E+00 0.0000E+00 0.0000E+00 0.0000E+00 0.0000E+00
21041  0.0000E+00 0.0000E+00 0.0000E+00 0.0000E+00 0.0000E+00 0.0000E+00
21051  0.0000E+00 0.0000E+00 0.0000E+00 0.0000E+00 0.0000E+00 0.0000E+00
21061  0.0000E+00 0.0000E+00 0.0000E+00 0.0000E+00 0.0000E+00 0.0000E+00
=
```

```
20100   U-235
20110   235.04 3.1000E-17 0.0000E+00 0.0000E+00 1.9290E+02
20101  6.0607E+00 1.3910E+00 3.1496E+00 1.2355E+00
20102  1.3493E+01 2.9359E+00 5.3492E+00 2.2024E+00
20103  3.7485E+01 2.4670E+01 4.0773E+01 1.6753E+01
20104  8.0454E+01 6.8163E+01 9.6498E+01 3.9649E+01
20105  6.8804E+01 5.5305E+01 1.0974E+02 4.5089E+01
20106  4.3674E+02 4.2200E+02 8.7811E+02 3.6080E+02
20111  6.8027E+00 1.5930E-01 1.5906E-03 1.1697E-06 0.0000E+00 0.0000E+00
20121  0.0000E+00 1.1080E+01 3.7459E-02 7.6640E-08 0.0000E+00 0.0000E+00
20131  0.0000E+00 0.0000E+00 1.2855E+01 1.5603E-02 0.0000E+00 0.0000E+00
20141  0.0000E+00 0.0000E+00 0.0000E+00 1.2291E+01 3.5879E-02 0.0000E+00
20151  0.0000E+00 0.0000E+00 0.0000E+00 0.0000E+00 1.3538E+01 0.0000E+00
20161  0.0000E+00 0.0000E+00 0.0000E+00 0.0000E+00 0.0000E+00 1.4784E+01
=
20200   U-238
20210   238.05 4.9000E-17 0.0000E+00 0.0000E+00 1.9390E+02
20201  6.1320E+00 2.3528E-01 3.8763E-01 1.4144E-01
20202  1.3160E+01 4.4233E-01 4.3791E-04 1.7562E-04
20203  3.5334E+01 8.0616E+00 6.8038E-04 2.7301E-04
20204  5.9006E+01 4.2350E+01 1.1417E-04 4.5814E-05
20205  9.6559E+00 5.2035E-01 5.0755E-06 2.0366E-06
20206  1.1115E+01 1.7866E+00 1.9225E-05 7.7145E-06
20211  8.1526E+00 1.1641E-01 2.0523E-04 3.2338E-08 0.0000E+00 0.0000E+00
20221  0.0000E+00 1.3208E+01 3.8851E-02 1.8712E-08 0.0000E+00 0.0000E+00
20231  0.0000E+00 0.0000E+00 2.7338E+01 1.0862E-02 0.0000E+00 0.0000E+00
20241  0.0000E+00 0.0000E+00 0.0000E+00 1.6681E+01 2.1347E-02 0.0000E+00
20251  0.0000E+00 0.0000E+00 0.0000E+00 0.0000E+00 9.1615E+00 0.0000E+00
20261  0.0000E+00 0.0000E+00 0.0000E+00 0.0000E+00 0.0000E+00 9.3552E+00
=
21900   H in H
21910     1.01 0.0000E+00 0.0000E+00 0.0000E+00 0.0000E+00
21901  2.6279E+00 4.2847E-05 0.0000E+00 0.0000E+00
21902  5.6138E+00 2.7828E-04 0.0000E+00 0.0000E+00
21903  6.7504E+00 3.3008E-03 0.0000E+00 0.0000E+00
21904  6.8308E+00 1.9491E-02 0.0000E+00 0.0000E+00
21905  9.3749E+00 5.1339E-02 0.0000E+00 0.0000E+00
21906  3.5919E+01 2.7204E-01 0.0000E+00 0.0000E+00
21911  3.6350E+00 2.0805E+00 1.4158E-01 5.3523E-04 3.5653E-05 9.1040E-06
21921  0.0000E+00 1.0699E+01 6.0448E+00 2.2770E-02 1.5822E-03 4.5117E-04
21931  0.0000E+00 0.0000E+00 1.6641E+01 3.3346E+00 2.3160E-01 6.6608E-02
21941  0.0000E+00 0.0000E+00 0.0000E+00 1.2990E+01 5.8081E+00 1.6705E+00
21951  0.0000E+00 0.0000E+00 0.0000E+00 0.0000E+00 1.1901E+01 9.5076E+00
21961  0.0000E+00 0.0000E+00 0.0000E+00 0.0000E+00 2.6123E-03 4.5132E+01
=
21400   B-10 i
21410    10.01 0.0000E+00 0.0000E+00 0.0000E+00 0.0000E+00
21401  3.1139E+00 7.4047E-01 0.0000E+00 0.0000E+00
21402  5.9263E+00 3.8014E+00 0.0000E+00 0.0000E+00
21403  3.9879E+01 3.7897E+01 0.0000E+00 0.0000E+00
21404  2.2711E+02 2.2512E+02 0.0000E+00 0.0000E+00
21405  5.9472E+02 5.9272E+02 0.0000E+00 0.0000E+00
21406  3.1425E+03 3.1405E+03 0.0000E+00 0.0000E+00
```

```
21411  2.5707E+00 1.3429E-01 5.8876E-07 4.2298E-10 0.0000E+00 0.0000E+00
21421  0.0000E+00 2.1300E+00 1.4011E-01 0.0000E+00 0.0000E+00 0.0000E+00
21431  0.0000E+00 0.0000E+00 2.0528E+00 7.1324E-02 0.0000E+00 0.0000E+00
21441  0.0000E+00 0.0000E+00 0.0000E+00 1.9803E+00 1.5967E-01 0.0000E+00
21451  0.0000E+00 0.0000E+00 0.0000E+00 0.0000E+00 2.1420E+00 0.0000E+00
21461  0.0000E+00 0.0000E+00 0.0000E+00 0.0000E+00 0.0000E+00 2.1447E+00
=
21500   B-11 i
21510    11.01 0.0000E+00 0.0000E+00 0.0000E+00 0.0000E+00
21501  2.7006E+00 2.1983E-05 0.0000E+00 0.0000E+00
21502  4.5939E+00 1.0195E-04 0.0000E+00 0.0000E+00
21503  4.5444E+00 5.3833E-05 0.0000E+00 0.0000E+00
21504  4.5447E+00 3.2315E-04 0.0000E+00 0.0000E+00
21505  4.5452E+00 8.5033E-04 0.0000E+00 0.0000E+00
21506  4.5489E+00 4.5026E-03 0.0000E+00 0.0000E+00
21511  2.8398E+00 1.8311E-01 6.0399E-07 9.5369E-11 0.0000E+00 0.0000E+00
21521  0.0000E+00 4.5820E+00 2.9308E-01 0.0000E+00 0.0000E+00 0.0000E+00
21531  0.0000E+00 0.0000E+00 4.6923E+00 1.4771E-01 0.0000E+00 0.0000E+00
21541  0.0000E+00 0.0000E+00 0.0000E+00 4.5099E+00 3.3012E-01 0.0000E+00
21551  0.0000E+00 0.0000E+00 0.0000E+00 0.0000E+00 4.8400E+00 0.0000E+00
21561  0.0000E+00 0.0000E+00 0.0000E+00 0.0000E+00 0.0000E+00 4.8400E+00
=
21300   Graphi
21310    12.00 0.0000E+00 0.0000E+00 0.0000E+00 0.0000E+00
21301  2.7262E+00 2.9526E-04 0.0000E+00 0.0000E+00
21302  4.3245E+00 1.9895E-06 0.0000E+00 0.0000E+00
21303  4.4676E+00 3.5257E-05 0.0000E+00 0.0000E+00
21304  4.4738E+00 1.9912E-04 0.0000E+00 0.0000E+00
21305  4.4862E+00 5.2560E-04 0.0000E+00 0.0000E+00
21306  4.8971E+00 2.7628E-03 0.0000E+00 0.0000E+00
21311  2.8272E+00 1.6624E-01 4.1165E-07 4.4114E-10 0.0000E+00 0.0000E+00
21321  0.0000E+00 4.3430E+00 2.6235E-01 0.0000E+00 0.0000E+00 0.0000E+00
21331  0.0000E+00 0.0000E+00 4.6003E+00 1.3331E-01 0.0000E+00 0.0000E+00
21341  0.0000E+00 0.0000E+00 0.0000E+00 4.4412E+00 2.9797E-01 0.0000E+00
21351  0.0000E+00 0.0000E+00 0.0000E+00 0.0000E+00 4.2713E+00 4.6719E-01
21361  0.0000E+00 0.0000E+00 0.0000E+00 0.0000E+00 1.0870E-03 4.8227E+00
=
21600   Nitrog
21610    14.00 0.0000E+00 0.0000E+00 0.0000E+00 0.0000E+00
21601  2.2405E+00 6.2591E-02 0.0000E+00 0.0000E+00
21602  6.0629E+00 1.9272E-03 0.0000E+00 0.0000E+00
21603  9.1781E+00 1.8792E-02 0.0000E+00 0.0000E+00
21604  9.5441E+00 1.1165E-01 0.0000E+00 0.0000E+00
21605  9.7376E+00 2.9390E-01 0.0000E+00 0.0000E+00
21606  1.1280E+01 1.5562E+00 0.0000E+00 0.0000E+00
21611  2.2691E+00 1.3443E-01 6.4465E-08 1.4511E-11 0.0000E+00 0.0000E+00
21621  0.0000E+00 6.0396E+00 4.0499E-01 0.0000E+00 0.0000E+00 0.0000E+00
21631  0.0000E+00 0.0000E+00 9.3853E+00 2.4057E-01 0.0000E+00 0.0000E+00
21641  0.0000E+00 0.0000E+00 0.0000E+00 9.3702E+00 5.3816E-01 0.0000E+00
21651  0.0000E+00 0.0000E+00 0.0000E+00 0.0000E+00 9.9201E+00 0.0000E+00
21661  0.0000E+00 0.0000E+00 0.0000E+00 0.0000E+00 0.0000E+00 1.0219E+01
=
21700   O-16 i
```

```
21710   15.99 0.0000E+00 0.0000E+00 0.0000E+00 0.0000E+00
21701  3.1936E+00 3.7994E-03 0.0000E+00 0.0000E+00
21702  3.6968E+00 1.8951E-06 0.0000E+00 0.0000E+00
21703  3.7237E+00 3.2499E-06 0.0000E+00 0.0000E+00
21704  3.7248E+00 1.1499E-05 0.0000E+00 0.0000E+00
21705  2.2125E+00 2.9595E-05 0.0000E+00 0.0000E+00
21706  3.8293E+00 1.5574E-04 0.0000E+00 0.0000E+00
21711  3.4298E+00 1.1314E-01 9.5813E-08 1.3458E-11 0.0000E+00 0.0000E+00
21721  0.0000E+00 3.6379E+00 1.6476E-01 0.0000E+00 0.0000E+00 0.0000E+00
21731  0.0000E+00 0.0000E+00 3.8021E+00 8.3211E-02 0.0000E+00 0.0000E+00
21741  0.0000E+00 0.0000E+00 0.0000E+00 3.7023E+00 1.8598E-01 0.0000E+00
21751  0.0000E+00 0.0000E+00 0.0000E+00 0.0000E+00 1.8966E+00 3.3528E-01
21761  0.0000E+00 0.0000E+00 0.0000E+00 0.0000E+00 9.7212E-04 3.9922E+00
=
22000   O-16 i
22010   15.99 0.0000E+00 0.0000E+00 0.0000E+00 0.0000E+00
22001  3.1936E+00 3.7994E-03 0.0000E+00 0.0000E+00
22002  3.6968E+00 1.8951E-06 0.0000E+00 0.0000E+00
22003  3.7237E+00 3.2499E-06 0.0000E+00 0.0000E+00
22004  3.7248E+00 1.1499E-05 0.0000E+00 0.0000E+00
22005  2.2125E+00 2.9595E-05 0.0000E+00 0.0000E+00
22006  3.8293E+00 1.5574E-04 0.0000E+00 0.0000E+00
22011  3.4298E+00 1.1314E-01 9.5813E-08 1.3458E-11 0.0000E+00 0.0000E+00
22021  0.0000E+00 3.6379E+00 1.6476E-01 0.0000E+00 0.0000E+00 0.0000E+00
22031  0.0000E+00 0.0000E+00 3.8021E+00 8.3211E-02 0.0000E+00 0.0000E+00
22041  0.0000E+00 0.0000E+00 0.0000E+00 3.7023E+00 1.8598E-01 0.0000E+00
22051  0.0000E+00 0.0000E+00 0.0000E+00 0.0000E+00 1.8966E+00 3.3528E-01
22061  0.0000E+00 0.0000E+00 0.0000E+00 0.0000E+00 9.7212E-04 3.9922E+00
=
21800   Argon
21810   39.95 0.0000E+00 0.0000E+00 0.0000E+00 0.0000E+00
21801  0.0000E+00 0.0000E+00 0.0000E+00 0.0000E+00
21802  0.0000E+00 0.0000E+00 0.0000E+00 0.0000E+00
21803  0.0000E+00 0.0000E+00 0.0000E+00 0.0000E+00
21804  0.0000E+00 0.0000E+00 0.0000E+00 0.0000E+00
21805  1.0204E-01 1.0204E-01 0.0000E+00 0.0000E+00
21806  5.4048E-01 5.4048E-01 0.0000E+00 0.0000E+00
21811  0.0000E+00 0.0000E+00 0.0000E+00 0.0000E+00 0.0000E+00 0.0000E+00
21821  0.0000E+00 0.0000E+00 0.0000E+00 0.0000E+00 0.0000E+00 0.0000E+00
21831  0.0000E+00 0.0000E+00 0.0000E+00 0.0000E+00 0.0000E+00 0.0000E+00
21841  0.0000E+00 0.0000E+00 0.0000E+00 0.0000E+00 0.0000E+00 0.0000E+00
21851  0.0000E+00 0.0000E+00 0.0000E+00 0.0000E+00 0.0000E+00 0.0000E+00
21861  0.0000E+00 0.0000E+00 0.0000E+00 0.0000E+00 0.0000E+00 0.0000E+00
=
22100  Void
22110  0.0000E+00 0.0000E+00 0.0000E+00 0.0000E+00 0.0000E+00
22101  7.1579E-03 0.0000E+00 0.0000E+00 0.0000E+00
22102  7.1579E-03 0.0000E+00 0.0000E+00 0.0000E+00
22103  7.1579E-03 0.0000E+00 0.0000E+00 0.0000E+00
22104  7.1579E-03 0.0000E+00 0.0000E+00 0.0000E+00
22105  7.1579E-03 0.0000E+00 0.0000E+00 0.0000E+00
22106  7.1579E-03 0.0000E+00 0.0000E+00 0.0000E+00
22111  0.0000E+00 0.0000E+00 0.0000E+00 0.0000E+00 0.0000E+00 0.0000E+00
```

```
22121  0.0000E+00 0.0000E+00 0.0000E+00 0.0000E+00 0.0000E+00 0.0000E+00
22131  0.0000E+00 0.0000E+00 0.0000E+00 0.0000E+00 0.0000E+00 0.0000E+00
22141  0.0000E+00 0.0000E+00 0.0000E+00 0.0000E+00 0.0000E+00 0.0000E+00
22151  0.0000E+00 0.0000E+00 0.0000E+00 0.0000E+00 0.0000E+00 0.0000E+00
22161  0.0000E+00 0.0000E+00 0.0000E+00 0.0000E+00 0.0000E+00 0.0000E+00
=
=      Compositions
=
30100  Boronated carbon bricks (1)
30101  3
30111  13 14 15
30121  7.29410E-2  6.56324E-4  2.64179E-3
=
30200  Top graphite reflector
30201  8
30211  13 14 15 16 17 18 19 20
30221  8.51462E-2 9.09725E-8 3.66176E-7 1.36389E-6
30222  3.65893E-7 8.15710E-9 3.00997E-8 1.50498E-8
=
30300  Cold helium chamber
30301  8
30311  13 14 15 16 17 18 19 20
30321  1.45350E-2 1.55296E-8 6.25088E-8 3.24753E-5
30322  8.71219E-6 1.94227E-7 7.16697E-7 3.58349E-7
=
30400  Top reflector
30401  8
30411  13 14 15 16 17 18 19 20
30421  8.02916E-2 8.59362E-8 3.45298E-7 3.50289E-6
30422  9.39723E-7 2.09498E-8 7.73051E-8 3.86526E-8
=
30500  Top core cavity
30501  6
30511  16 17 18 19 20 21
30521  3.88795E-5 1.04303E-5 2.32528E-7 8.58030E-7
30522  4.29015E-7 1.0 ! Moist air at 15 C
=
30600  Dummy balls simplified (1)
30601  8
30611  13 14 15 16 17 18 19 20
30621  5.72501E-2 6.14369E-9 2.47292E-8 1.51630E-5
30622  4.06779E-6 9.06859E-8 3.34631E-7 1.67316E-7
=
30700  Dummy balls simplified (2)
30701  8
30711  13 14 15 16 17 18 19 20
30721  5.72501E-2 6.14369E-9 2.47292E-8 1.51630E-5
30722  4.06779E-6 9.06859E-8 3.34631E-7 1.67316E-7
=
30800  Bottom reflector structures (1)
30801  8
30811  13 14 15 16 17 18 19 20
30821  7.81408E-2 8.34879E-8 3.36049E-7 4.45053E-6
```

```
30822  1.19395E-6 2.66175E-8 9.82187E-8 4.91093E-8
=
30900  Bottom reflector structures (2)
30901  8
30911  13 14 15 16 17 18 19 20
30921  8.23751E-2 8.80119E-8 3.54259E-7 2.58488E-6
30922  6.93448E-7 1.54595E-8 5.70456E-8 2.85228E-8
=
31000  Bottom reflector structures (3)
31001  8
31011  13 14 15 16 17 18 19 20
31021  8.43647E-2 5.94023E-5 2.39102E-4 1.57694E-6
31022  4.23047E-7 9.43126E-9 3.48014E-8 1.74007E-8
=
31100  Bottom reflector structures (4)
31101  8
31111  13 14 15 16 17 18 19 20
31121  8.17101E-2 3.11268E-5 1.25289E-4 2.80916E-6
31122  7.53616E-7 1.68008E-8 6.19952E-8 3.09976E-8
=
31200  Bottom reflector structures (5)
31201  8
31211  13 14 15 16 17 18 19 20
31221  8.50790E-2 4.16093E-5 1.67483E-4 1.30161E-6
31222  3.49184E-7 7.78458E-9 2.87252E-8 1.43626E-8
=
31300  Bottom reflector structures (6)
31301  8
31311  13 14 15 16 17 18 19 20
31321  8.19167E-2 7.13473E-6 2.87182E-5 2.77125E-6
31322  7.43445E-7 1.65741E-8 6.11585E-8 3.05793E-8
=
31400  Bottom reflector structures (7)
31401  8
31411  13 14 15 16 17 18 19 20
31421  5.41118E-2 1.14914E-5 4.62542E-5 1.50124E-5
31422  4.02740E-6 8.97853E-8 3.31308E-7 1.65654E-7
=
31500  Bottom reflector structures (8)
31501  8
31511  13 14 15 16 17 18 19 20
31521  3.32110E-2 3.54835E-8 1.42826E-7 2.42467E-5
31522  6.50468E-6 1.45013E-7 5.35099E-7 2.67549E-7
=
31600  Bottom reflector structures (9)
31601  3
31611  13  14  15
31621  8.81811E-2  7.14143E-6  2.87452E-5
=
31700  Boronated carbon bricks (2)
31701  3
31711  13  14  15
31721  7.65984E-2  6.89235E-4  2.77426E-3
```

```
=
31800   Carbon bricks (1)
31801   1
31811   13
31821   7.97184E-2
=
31900   Boronated carbon bricks (3)
31901   3
31911   13  14  15
31921   7.61157E-2  6.84890E-4  2.75677E-3
=
32000   Graphite reflector structure (1)
32001   8
32011   13 14 15 16 17 18 19 20
32021   8.78374E-2 9.38478E-8 3.77749E-7 1.78179E-7
32022   4.78003E-8 1.06564E-9 3.93223E-9 1.96612E-9
=
32100   Graphite reflector structure (2)
32101   8
32111   13 14 15 16 17 18 19 20
32121   5.79696E-2 6.19364E-8 2.49302E-7 1.33380E-5
32122   3.57820E-6 7.97711E-8 2.94359E-7 1.47180E-7
=
32200   Graphite reflector structure (3)
32201   3
32211   13  14  15
32221   8.82418E-2  9.42800E-8  3.79489E-7
=
32300   Graphite reflector structure (4)
32301   3
32311   13  14  15
32321   8.82418E-2  9.42800E-8  3.79489E-7
=
32400   Graphite reflector structure (5)
32401   8
32411   13 14 15 16 17 18 19 20
32421   8.79541E-2 3.35054E-5 1.34864E-4 5.27856E-8
32422   1.41609E-8 3.15697E-10 1.16492E-9 5.82462E-10
=
32500   Graphite reflector structure (6)
32501   3
32511   13  14  15
32521   8.82418E-2  9.42800E-8  3.79489E-7
=
32600   Graphite reflector structure (7)
32601   8
32611   13 14 15 16 17 18 19 20
32621   8.46754E-2 9.04696E-8 3.64151E-7 1.57136E-6
32622   4.21552E-7 9.39792E-9 3.46784E-8 1.73392E-8
=
32700   Boronated carbon bricks (4)
32701   3
32711   13  14  15
```

```
32721   5.89319E-2  5.30271E-4  2.13441E-3
=
32800   Graphite reflector structure (8)
32801   8
32811   13 14 15 16 17 18 19 20
32821   6.78899E-2 2.78600E-6 1.12140E-5 8.96110E-6
32822   2.40400E-6 5.35940E-8 1.97762E-7 9.88811E-8
=
32900   Graphite reflector structure (9)
32901   8
32911   13 14 15 16 17 18 19 20
32921   4.03794E-2 2.78600E-6 1.12140E-5 2.10822E-5
32922   5.65574E-6 1.26087E-7 4.65262E-7 2.32631E-7
=
33000   Graphite reflector structure (10)
33001   8
33011   13 14 15 16 17 18 19 20
33021   6.78899E-2 7.25335E-8 2.91965E-7 8.52248E-6
33022   2.28634E-6 5.09708E-8 1.88082E-7 9.40412E-8
=
33100   Graphite reflector, control rod borings region
33101   8
33111   13 14 15 16 17 18 19 20
33121   6.34459E-2 6.76727E-8 2.72853E-7 1.09251E-5
33122   2.93090E-6 6.53404E-8 2.41106E-7 1.20553E-7
=
34100   Graphite reflector structure (11)
34101   8
34111   13 14 15 16 17 18 19 20
34121   6.78899E-2 7.25335E-8 2.91965E-7 8.52248E-6
34122   2.28634E-6 5.09708E-8 1.88082E-7 9.40412E-8
=
34200   Graphite reflector structure (12)
34201   8
34211   13 14 15 16 17 18 19 20
34221   6.76758E-2 2.49409E-5 1.00390E-4 9.00634E-6
34222   2.41614E-6 5.38646E-8 1.98761E-7 9.93804E-8
=
34300   Graphite reflector structure (13)
34301   8
34311   13 14 15 16 17 18 19 20
34321   8.61476E-2 6.77874E-8 2.72853E-7 9.22759E-7
34322   2.47550E-7 5.51879E-9 2.03643E-8 1.01822E-8
=
34400   Graphite reflector structure (14)
34401   8
34411   13 14 15 16 17 18 19 20
34421   8.29066E-2 8.85797E-8 3.56544E-7 2.35070E-6
34422   6.30625E-7 1.40589E-8 5.18775E-8 2.59388E-8
=
34500   Graphite reflector structure (15)
34501   8
34511   13 14 15 16 17 18 19 20
```

```
34521  8.61476E-2 6.77874E-8 2.72853E-7 9.22759E-7
34522  2.47550E-7 5.51879E-9 2.03643E-8 1.01822E-8
=
34600  Boronated carbon bricks (5)
34601  3
34611  13  14  15
34621  7.47805E-2  6.72877E-4  2.70841E-3
=
34700  Carbon bricks (2)
34701  1
34711  13
34721  7.78265E-2
=
34800  Graphite reflector structure (16)
34801  3
34811  13  14  15
34821  8.82418E-2  9.42800E-8  3.79489E-7
=
34900  Graphite reflector structure (17)
34901  3
34911  13  14  15
34921  8.82418E-2  9.42800E-8  3.79489E-7
=
35000  Graphite reflector structure (18)
35001  3
35011  13  14  15
35021  8.82418E-2  9.42800E-8  3.79489E-7
=
35100  Graphite reflector structure (19)
35101  8
35111  13 14 15 16 17 18 19 20
35121  8.79541E-2 3.35054E-5 1.34864E-4 5.27856E-8
35122  1.41609E-8 3.15697E-10 1.16492E-9 5.82462E-10
=
35200  Graphite reflector structure (20)
35201  3
35211  13  14  15
35221  8.82418E-2  9.42800E-8  3.79489E-7
=
35300  Graphite reflector structure (21)
35301  8
35311  13 14 15 16 17 18 19 20
35321  8.55860E-2 9.14425E-8 3.68068E-7 1.17015E-6
35322  3.13917E-7 6.99836E-9 2.58240E-8 1.29120E-8
=
35400  Graphite reflector structure (22)
35401  3
35411  13  14  15
35421  8.82418E-2  9.42800E-8  3.79489E-7
=
35500  Boronated carbon bricks (6)
35501  3
35511  13  14  15
```

```
35521  7.65984E-2  6.89235E-4  2.77426E-3
=
35600  Carbon bricks (3)
35601  1
35611  13
35621  7.97184E-2
=
35700  Graphite reflector structure (23)
35701  8
35711  13 14 15 16 17 18 19 20
35721  7.28262E-2 7.78096E-8 3.13193E-7 6.79213E-6
35722  1.82213E-6 4.06220E-8 1.49895E-7 7.49476E-8
=
35800  Graphite reflector, cold He flow region (1)
35801  8
35811  13 14 15 16 17 18 19 20
35821  7.60368E-2 8.12398E-8 3.27000E-7 5.37755E-6
35822  1.44264E-6 3.21617E-8 1.18677E-7 5.93385E-8
=
35900  Graphite reflector, cold He flow region (2)
35901  8
35911  13 14 15 16 17 18 19 20
35921  7.60368E-2 8.12398E-8 3.27000E-7 5.37755E-6
35922  1.44264E-6 3.21617E-8 1.18677E-7 5.93385E-8
=
36000  Graphite reflector, cold He flow region (3)
36001  8
36011  13 14 15 16 17 18 19 20
36021  7.57889E-2 2.88713E-5 1.16211E-4 5.42301E-6
36022  1.45484E-6 3.24336E-8 1.19680E-7 5.98401E-8
=
36100  Graphite reflector, cold He flow region (4)
36101  8
36111  13 14 15 16 17 18 19 20
36121  7.60368E-2 8.12398E-8 3.27000E-7 5.37755E-6
36122  1.44264E-6 3.21617E-8 1.18677E-7 5.93385E-8
=
36200  Graphite reflector, cold He flow region (5)
36201  8
36211  13 14 15 16 17 18 19 20
36221  7.37484E-2 7.87948E-8 3.17159E-7 6.38580E-6
36222  1.71313E-6 3.81919E-8 1.40928E-7 7.04641E-8
=
36300  Graphite reflector, cold He flow region (6)
36301  8
36311  13 14 15 16 17 18 19 20
36321  7.60368E-2 8.12398E-8 3.27000E-7 5.37755E-6
36322  1.44264E-6 3.21617E-8 1.18677E-7 5.93385E-8
=
36400  Boronated carbon bricks (7)
36401  3
36411  13  14  15
36421  6.60039E-2  5.93904E-4  2.39054E-3
```

```
=
36500  Carbon bricks (4)
36501  1
36511  13
36521  6.86924E-2
=
36600  Graphite reflector structure (24)
36601  8
36611  13 14 15 16 17 18 19 20
36621  5.82699E-2 6.22572E-8 2.50593E-7 1.32057E-5
36622  3.54270E-6 7.89797E-8 2.91435E-7 1.45718E-7
=
36700  Graphite reflector structure (25)
36701  3
36711  13  14  15
36721  8.82418E-2  9.42800E-8  3.79489E-7
=
36800  Graphite reflector structure (26)
36801  8
36811  13 14 15 16 17 18 19 20
36821  8.79541E-2 3.35054E-5 1.34864E-4 5.27856E-8
36822  1.41609E-8 3.15697E-10 1.16492E-9 5.82462E-10
=
36900  Graphite reflector structure (27)
36901  3
36911  13  14  15
36921  8.82418E-2  9.42800E-8  3.79489E-7
=
37000  Graphite reflector structure (28)
37001  8
37011  13 14 15 16 17 18 19 20
37021  8.61500E-2 9.20451E-8 3.70493E-7 9.21653E-7
37022  2.47253E-7 5.51217E-9 2.03399E-8 1.01700E-8
=
37100  Graphite reflector structure (29)
37101  3
37111  13  14  15
37121  8.82418E-2  9.42800E-8  3.79489E-7
=
37200  Boronated carbon bricks (8)
37201  3
37211  13  14  15
37221  7.65984E-2  6.89235E-4  2.77426E-3
=
37300  Carbon bricks (5)
37301  1
37311  13
37321  7.97184E-2
=
37400  Boronated carbon bricks (9)
37401  3
37411  13  14  15
37421  7.65984E-2  6.89235E-4  2.77426E-3
```

```
=
37500  Boronated carbon bricks (10)
37501  3
37511  13  14  15
37521  7.65984E-2  6.89235E-4  2.77426E-3
=
37600  Boronated carbon bricks (11)
37601  3
37611  13  14  15
37621  7.65984E-2  6.89235E-4  2.77426E-3
=
37700  Boronated carbon bricks (12)
37701  3
37711  13  14  15
37721  7.49927E-2  6.74785E-4  2.71609E-3
=
37800  Boronated carbon bricks (13)
37801  3
37811  13  14  15
37821  7.65984E-2  6.89235E-4  2.77426E-3
=
37900  Boronated carbon bricks (14)
37901  3
37911  13  14  15
37921  7.65984E-2  6.89235E-4  2.77426E-3
=
38000  Graphite reflector structure (30)
38001  3
38011  13  14  15
38021  8.82418E-2  9.42800E-8  3.79489E-7
=
38100  Dummy balls taken as carbon bricks
38101  6
38111  13 16 17 18 19 20
38121  8.47872E-2 3.75543E-6 1.00747E-6 2.24603E-8
38122  8.28784E-8 4.14392E-8
=
38200  Graphite reflector structure (31)
38201  8
38211  13 14 15 16 17 18 19 20
38221  6.78899E-2 2.78600E-6 1.12140E-5 8.96110E-6
38222  2.40400E-6 5.35940E-8 1.97762E-7 9.88811E-8
=
38300  Bottom reflector with hot He flow borings (1)
38301  8
38311  13 14 15 16 17 18 19 20
38321  8.51047E-2 9.09283E-8 3.65998E-7 1.38221E-6
38322  3.70808E-7 8.26665E-9 3.05040E-8 1.52520E-8
=
38400  Bottom reflector with hot He flow borings (2)
38401  8
38411  13 14 15 16 17 18 19 20
38421  8.51047E-2 9.09283E-8 3.65998E-7 1.38221E-6
```

```
38422  3.70808E-7 8.26665E-9 3.05040E-8 1.52520E-8
=
38500  Bottom reflector with hot He flow borings (3)
38501  8
38511  13 14 15 16 17 18 19 20
38521  8.51047E-2 9.09283E-8 3.65998E-7 1.38221E-6
38522  3.70808E-7 8.26665E-9 3.05040E-8 1.52520E-8
=
38600  Bottom reflector with hot He flow borings (4)
38601  8
38611  13 14 15 16 17 18 19 20
38621  8.51047E-2 9.09283E-8 3.65998E-7 1.38221E-6
38622  3.70808E-7 8.26665E-9 3.05040E-8 1.52520E-8
=
38700  Bottom reflector with hot He flow borings (5)
38701  8
38711  13 14 15 16 17 18 19 20
38721  8.51047E-2 9.09283E-8 3.65998E-7 1.38221E-6
38722  3.70808E-7 8.26665E-9 3.05040E-8 1.52520E-8
=
38800  Bottom reflector with hot He flow borings (6)
38801  8
38811  13 14 15 16 17 18 19 20
38821  8.51047E-2 9.09283E-8 3.65998E-7 1.38221E-6
38822  3.70808E-7 8.26665E-9 3.05040E-8 1.52520E-8
=
38900  Bottom reflector with hot He flow borings (7)
38901  8
38911  13 14 15 16 17 18 19 20
38921  8.51047E-2 9.09283E-8 3.65998E-7 1.38221E-6
38922  3.70808E-7 8.26665E-9 3.05040E-8 1.52520E-8
=
39000  Bottom reflector with hot He flow borings (8)
39001  8
39011  13 14 15 16 17 18 19 20
39021  8.51047E-2 9.09283E-8 3.65998E-7 1.38221E-6
39022  3.70808E-7 8.26665E-9 3.05040E-8 1.52520E-8
=
39100  Dummy balls simplified (3)
39101  8
39111  13 14 15 16 17 18 19 20
39121  5.72501E-2 6.14369E-9 2.47292E-8 1.51630E-5
39122  4.06779E-6 9.06859E-8 3.34631E-7 1.67316E-7
=
39200  Dummy balls simplified (4)
39201  8
39211  13 14 15 16 17 18 19 20
39221  5.72501E-2 6.14369E-9 2.47292E-8 1.51630E-5
39222  4.06779E-6 9.06859E-8 3.34631E-7 1.67316E-7
=
39300  Dummy balls simplified (5)
39301  8
39311  13 14 15 16 17 18 19 20
```

```
39321  5.72501E-2 6.14369E-9 2.47292E-8 1.51630E-5
39322  4.06779E-6 9.06859E-8 3.34631E-7 1.67316E-7
=
39400  Dummy balls simplified (6)
39401  8
39411  13 14 15 16 17 18 19 20
39421  5.72501E-2 6.14369E-9 2.47292E-8 1.51630E-5
39422  4.06779E-6 9.06859E-8 3.34631E-7 1.67316E-7
=
39500  Dummy balls simplified (7)
39501  8
39511  13 14 15 16 17 18 19 20
39521  5.72501E-2 6.14369E-9 2.47292E-8 1.51630E-5
39522  4.06779E-6 9.06859E-8 3.34631E-7 1.67316E-7
=
39600  Dummy balls simplified (8)
39601  8
39611  13 14 15 16 17 18 19 20
39621  5.72501E-2 6.14369E-9 2.47292E-8 1.51630E-5
39622  4.06779E-6 9.06859E-8 3.34631E-7 1.67316E-7
=
39700  Dummy balls simplified (9)
39701  8
39711  13 14 15 16 17 18 19 20
39721  5.72501E-2 6.14369E-9 2.47292E-8 1.51630E-5
39722  4.06779E-6 9.06859E-8 3.34631E-7 1.67316E-7
=
39800  Dummy balls simplified (10)
39801  8
39811  13 14 15 16 17 18 19 20
39821  5.72501E-2 6.14369E-9 2.47292E-8 1.51630E-5
39822  4.06779E-6 9.06859E-8 3.34631E-7 1.67316E-7
=
39900  Mixture balls
39901  12
39911  1  2  3  4  5  6  7  8
39912  9 10 11 12
39921  6.69520E-6 3.22755E-5 7.79414E-5 8.51054E-5
39922  5.40964E-2 9.92089E-9 3.99328E-8 1.55875E-5
39923  4.09021E-6 9.11929E-8 3.34631E-7 1.67316E-7
.
```

APPENDIX B
CALCULATION OF BASE-CASE ATOMIC NUMBER DENSITIES IN THE CORE REGION

This appendix presents the calculation of the atomic number densities for Region 99 in the PEBBED model, which is the core region, where the mixture of fuel and dummy balls is located.

First, some data from Table 3 are repeated:

Fuel enrichment = 17% by weight
Core unit cell volume = 185.405 cm^3
Kernel density = 10.4 g/cm^3
Buffer layer density = 1.1 g/cm^3
IPyC density = 1.9 g/cm^3
SiC density = 3.18 g/cm^3
OPyC density = 1.9 g/cm^3
Fuel matrix density = 1.73 g/cm^3
Dummy matrix density = 1.84 g/cm^3
Pebble packing fraction = 61%
Fuel loading per fuel pebble = 5 g U
Number of kernels in a fuel pebble = 8335
Ratio of fuel pebbles to dummy pebbles: 57:43
Boron concentration in kernel (by weight) = 4 ppm
Boron concentration in fuel matrix (by weight) = 1.3 ppm
Boron concentration in dummy-ball matrix (by weight) = 0.125 ppm
Kernel radius = 0.025 cm
Buffer layer thickness = 0.009 cm
IPyC layer thickness = 0.004 cm
SiC layer thickness = 0.0035 cm
OPyC layer thickness = 0.004 cm

The weights of one gram-mole of the nuclides and elements used in the calculations are taken from the Chart of the Nuclides.[B1]

B.1 Nuclides in kernel

The uranium is 17% U-235 by weight. Ignore all isotopes except U-235 and U-238. Let $\tilde{N}_{235}$ and $\tilde{N}_{238}$ be the atom fractions of U-235 and U-238, respectively, A_{235} and A_{238} be the

molecular weights of U-235 and U-238, respectively, and $\overline{A}$ be the average molecular weight of the mixture of the two isotopes. Then

$$0.17\overline{A} = \tilde{N}_{235}A_{235}$$

and $0.83\overline{A} = \tilde{N}_{238}A_{238}$,

so that $\frac{0.17\overline{A}}{0.83\overline{A}} = \frac{\tilde{N}_{235}A_{235}}{\tilde{N}_{238}A_{238}} = \frac{\tilde{N}_{235}x235.043928}{\tilde{N}_{238}x238.050788}$,

or $\frac{\tilde{N}_{235}}{\tilde{N}_{238}} = 0.207439$.

But $\tilde{N}_{235} + \tilde{N}_{238} = 1$. This and the previous equation are solved simultaneously to yield

$$\tilde{N}_{235} = 0.171801$$

and $\tilde{N}_{238} = 0.828199$.

The mass of uranium in an average UO_2 molecule is

(0.171801x235.043928 + 0.828199x238.050788)(g/mole)x 1 mole/6.022x10^{23} molecules = 3.94444x10^{-22} g.

The ratio of fuel balls to dummy balls is 57:43. Thus, the computational cell is defined to contain 57% of a fuel ball and 43% of a dummy ball, plus the volume of coolant associated with one ball in the core. The number of U atoms, or UO_2 molecules, in a computational cell is thus

$(N_U)_{cell}$ = 0.57x5 g/3.94444x10^{-22} g/molecule = 7.22536x10^{21} molecules.

Then the atomic number densities are

$(n_{U\text{-}235})_{cell}$ = 0.171801 x 7.22536x10^{21} x 10^{-24}/185.405 a/b-cm = 6.69520x10^{-6}a/b-cm

and, analogously, $(n_{U\text{-}238})_{cell}$ = 3.22755x10^{-5} a/b-cm

and $(\overline{n}_O)_{cell}^{kernels} = 7.79414x10^{-5}$ a/b-cm.

The oxygen in the kernel is given a different material label from the oxygen in the water vapor in the PEBBED and COMBINE inputs because the cross sections are different in different

materials. Similarly, identical nuclides in the core and reflector are given different labels because their cross sections will be different in the two spectral zones.

The boron concentration in the kernel is 4 ppm by weight of uranium. The mass of the average boron atom is (10.811g/mole)/6.022x10^{23} atoms/mole) = 1.79525x10^{-23} g/atom. Then the ratio of the number of boron atoms to the number of UO_2 molecules is

$$\frac{4x10^{-6}\,x\,3.94444x10^{-22}}{1.79525x10^{-23}} = 8.78861x10^{-5}$$

and the number of atoms of boron in the computational cell from kernels is

$$(N_B)_{cell}^{kernels} = 8.78861x10^{-5}(N_U)_{cell} = 6.35009x10^{17}\,\text{atoms}.$$

B.2 Nuclides in fuel particle layers

The number of TRISO particles in the cell is 0.57x8335=4751. The volume of the buffer layer is $4\pi[(0.025 + 0.009)^3 - 0.025^3]/3$ cm^3 = 9.91864x10^{-5} cm^3, so the total volume of buffer zone in the cell is 4751 x 9.91864x10^{-5} cm^3 = 0.471235 cm^3. The density of the buffer zone is 1.1 g/cm^3, and the boron content is 1.3 ppm (by weight).

The masses of the average carbon and boron atoms are 12.011/6.022x10^{23} g = 1.99452x10^{-23} g and 10.811/6.022x10^{23} g = 1.79525x10^{-23} g, respectively; by number, a boron content of 1.3 ppm by mass is

1.3x10^{-6} x 12.011/10.811 = 1.44430x10^{-6}.

Then $(n_C)_{buffer}$ = 1.1 g/cm^3 / (1.99452x10^{-23} + 1.4443x10^{-6} x 1.79525x10^{-23}) g = 5.51510x10^{22} atoms/cm^3

and the total number of C atoms in the cell from buffer zones is

$$(N_C)_{cell}^{buffer} = 5.51510x10^{22}\,\text{atoms}/cm^3\,x\,0.471235\,cm^3 = 2.59891x10^{22}\,\text{atoms}.$$

It is assumed that the graphite in the carbon layers of the TRISO particle have the same boron concentration as the graphite fuel matrix. This assumption can only affect the boron content of the computational cell slightly. The number of boron atoms in the cell from buffer zones is

$$(N_B)_{cell}^{buffer} = 1.4443x10^{-6}\,x\,2.59891x10^{22}\,\text{atoms}=3.75361x10^{16}\,\text{atoms}\ .$$

In similar fashion, the carbon, silicon, and boron contents of the remaining zones are found. The

silicon carbide layer is assumed to contain no boron.

$(N_C)_{cell}^{IPyC} = 2.95135x10^{22}$ atoms

$(N_B)_{cell}^{IPyC} = 4.26264x10^{16}$ atoms

$(N_C)_{cell}^{SiC} = 1.57790x10^{22}$ atoms

$(N_{Si})_{cell}^{SiC} = 1.57790x10^{22}$ atoms

$(N_C)_{cell}^{OPyC} = 4.30778x10^{22}$ atoms

$(N_B)_{cell}^{OPyC} = 6.22173x10^{16}$ atoms

B.3 Nuclides in fuel matrix and dummy-ball matrix

The total volume of TRISO particles in the cell is $4751x4\pi(0.0455\text{ cm})^3/3 = 1.87460\text{ cm}^3$. The volume of one pebble is $4\pi(3\text{ cm})^3/3 = 113.097\text{ cm}^3$, of which in the computational cell 57% is fuel pebble and 43% is dummy pebble. Then the volume of fuel matrix in the cell is $0.57x113.097\text{ cm}^3 - 1.87460\text{ cm}^3 = 62.5907\text{ cm}^3$, and the volume of dummy matrix in the cell is $0.43x113.097\text{ cm}^3 = 48.6317\text{ cm}^3$. From the given densities of the graphite matrix in the fuel and dummy balls, 1.73 g/cm^3 and 1.84 g/cm^3, respectively, and the mass of the average carbon atom, it is found that the atomic number densities of carbon in the fuel and dummy matrix materials are $8.67377x10^{22}$ atoms/cm^3 and $9.22528x10^{22}$ atoms/cm^3, respectively. Then the carbon atomic number densities are

$(N_C)_{cell}^{fuel\ matrix} = 5.42897x10^{24}$ atoms

and

$(N_C)_{cell}^{dummy\ matrix} = 4.48641x10^{24}$ atoms .

In the fuel matrix the boron concentration is 1.3 ppm, but in the dummy matrix it is 0.125 ppm by weight, which is equivalent to 0.138875 ppm by number. These proportions give the boron content of the matrix materials:

$(N_B)_{cell}^{fuel\ matrix} = 7.84269x10^{18}$ atoms

and

$(N_B)_{cell}^{dummy\ matrix} = 6.23050x10^{17}$ atoms .

B.4 Total carbon and boron number densities

When all the contributions to the carbon and boron contents of the cell are summed and divided by the cell volume, and the result is converted to a/b-cm, the resulting densities are

$(\overline{n}_C)_{cell} = 5.40964x10^{-2}$ a/b-cm

$(\overline{n}_{B-10})_{cell} = 9.92089x10^{-9}$ a/b-cm

and

$(\overline{n}_{B-11})_{cell} = 3.99328x10^{-8}$ a/b-cm .

B.5 Nuclides in air

The densities of the gaseous constituents are found from the specified conditions and the assumption that the air is saturated with water vapor. At 15 °C (288.15 K), at a relative humidity of 100% the water vapor density is[B2] 1.28343x10^{-5} g/cm^3 and the vapor pressure is 1.70507x10^{-3} MPa. (Reference B2 gives data in British units; 15 °C = 59 °F, at which the saturation pressure is 0.2473 lbf/in^2 (psi) and the saturated vapor specific volume is 1248.1 ft^3/lbm. The conversion factors used to obtain metric units are[B3] 6894.7572 N/m^2-psi and 16.018463 kg-ft^3/lbm-m^3) At this mass density, the number density of water vapor molecules is found to be 4.29014x10^{17} molecules/cm^3, and the average number densities of hydrogen and oxygen from vapor in the cell are

$(\overline{n}_H)_{cell} = 3.34631x10^{-7}$ a/b-cm

and

$(\overline{n}_O)_{cell}^{vapor} = 1.67316x10^{-7}$ a/b-cm .

The pressure of the dry air is then 0.1013 MPa – 1.70507x10^{-3} MPa = 9.95949x10^{-2} MPa. The ideal gas law (with R = 8.314 Pa-m^3/mole-K)[B4] then gives a molecular density of 2.50351x10^{19} molecules/cm^3. The proportions given in subsection 3.1.3 lead to the following atomic densities:

$(\overline{n}_N)_{cell} = 1.55875x10^{-5}$ a/b-cm

$(\overline{n}_O)_{cell}^{air} = 4.09021x10^{-6}$ a/b-cm

$(\overline{n}_{Ar})_{cell} = 9.11929x10^{-8}$ a/b-cm

REFERENCES FOR APPENDIX B

B1. *Chart of the Nuclides*, Thirteenth Edition, General Electric Company, 1984.

B2. Joseph H. Keenan and Frederick G. Keyes, *Thermodynamic Properties of Steam*, Wiley, New York, Thirty-fifth Printing, 1963.

B3. Donald R. Pitts and Leighton E. Sissom, *Heat Transfer*, Schaum's Outline Series in Engineering, McGraw-Hill, New York, 1977.

B4. Samuel Glasstone and Alexander Sesonske, *Nuclear Reactor Engineering*, Third Edition, Van Nostrand Reinhold, New York, 1981.

APPENDIX C

NUCLEAR CONSTANTS

Avogadro's Number $6.022 \times 10^{23} \frac{\text{atoms}}{\text{gram} - \text{mole}}$

TABLE C1. Atomic Weights.

Nuclide or Isotope	Atomic Weight
H	1.00794
Li	6.941
B	10.811
^{10}B	10.0129
^{11}B	11.0093
C	12.011
O	15.9994
Si	28.0855
^{235}U	235.043928
^{238}U	238.050788

[2] "Chart of the Nuclides," Thirteenth Edition, General Electric Company, 1984.